Bochum, June 6th, 2019

How U-Pb dating of calcite veins and calcite twinning / stylolite roughness paleopiezometry help unravel complex thrust sequence and stress evolution in orogenic forelands : A case study in the Laramide province (Bighorn basin, Wyoming, USA)

Olivier LACOMBE

Collaboration with
Nicolas BEAUDOIN, Khalid AMROUCH (former PhD students)
Nicolas BELLAHSEN … and many others

SCIENCES SORBONNE UNIVERSITÉ
ISTeP Institut des Sciences de la Terre de Paris UMR 7193 - SU - CNRS
cnrs INSU Observer & comprendre

Thick-skinned deformation in orogenic forelands : what we know

In thick-skinned (i.e., basement-involved) FTBs, shortening involves a significant part of the crust above a deep ductile detachment (≠ thin-skinned)

A key process by which basement becomes involved is the inversion of pre-existing extensional faults

Basement-involvement in FTBs requires a significant degree of mechanical coupling between the orogen and the foreland and far-field orogenic stress transmission through the crust and/or mantle lithosphere

Basement involvement in FTBs requires a generally rather hot, hence mechanically weak lithosphere

Orogenic forelands may have a complex, polyphase evolution, with implication of different structural styles

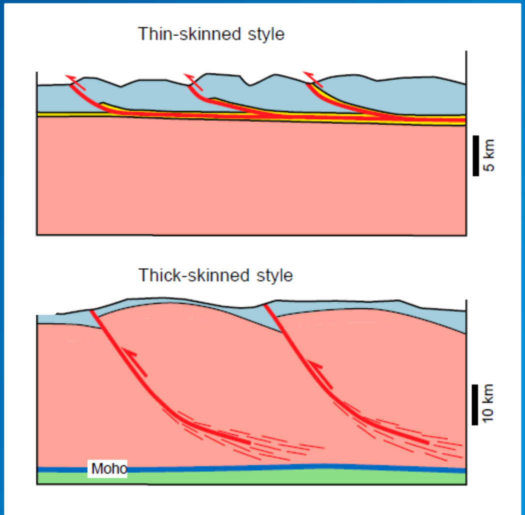

Pfiffner, 2017

Pending questions to be addressed today :

* How does deformation propagate and distribute during thick-skinned deformation ?

* How does stress (orientation / magnitude) distribute and evolve during thick-skinned deformation ?

*Are sequence of deformation and orogenic stress transmission similar for thick-skinned and thin-skinned tectonics ?

*Side question : to what extent micro/meso-scale observations are relevant to large-scale tectonics ?

Q1 : How are orogenic stresses transmitted into the foreland ?

Calcite twinning analyses support a decrease of differential stress magnitudes with increasing distance to the hinterland-foreland boundary

(Hnat et al., 2013; Van der Pluijm et al., 1997) (Lacombe et al., 2007) (Xypolias & Koukouvelas, 2005)

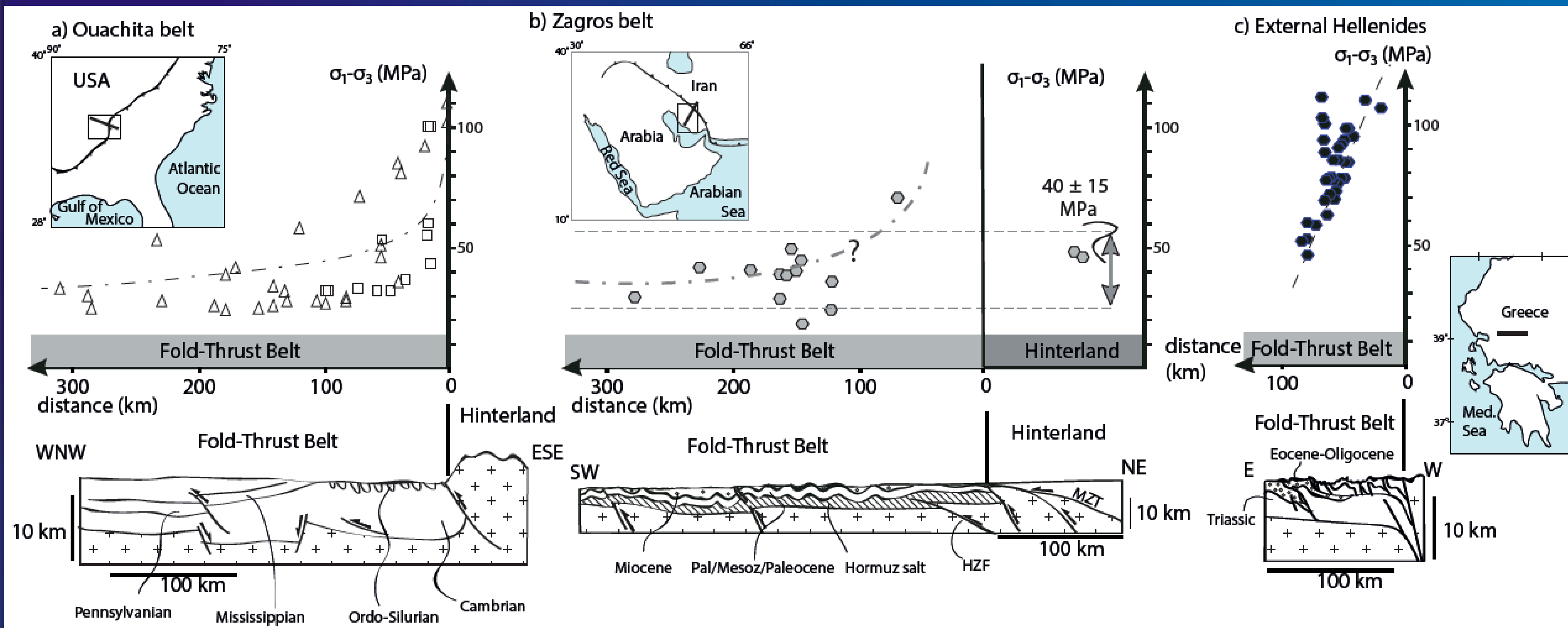

(Beaudoin and Lacombe, 2018)

… and also in the north Pyrenean foreland (Lacombe et al., 1996; Rocher et al., 2000)…

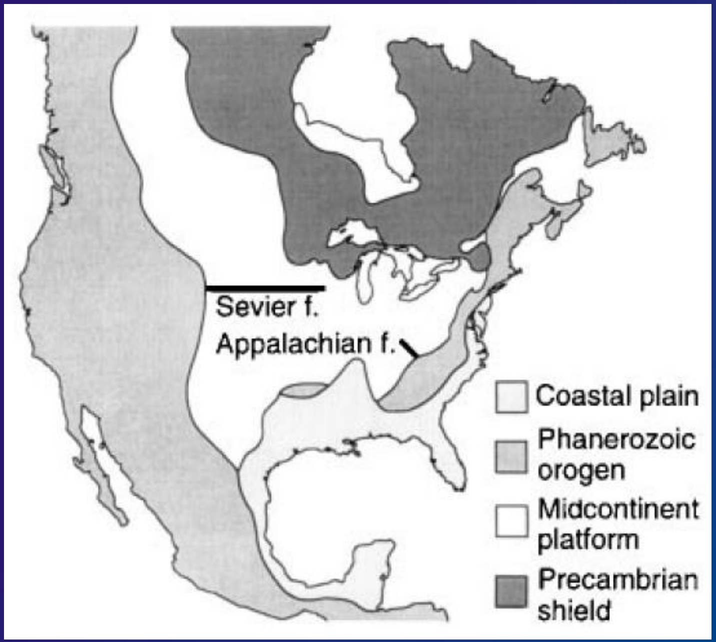

(Van der Puijm et al., 1997)

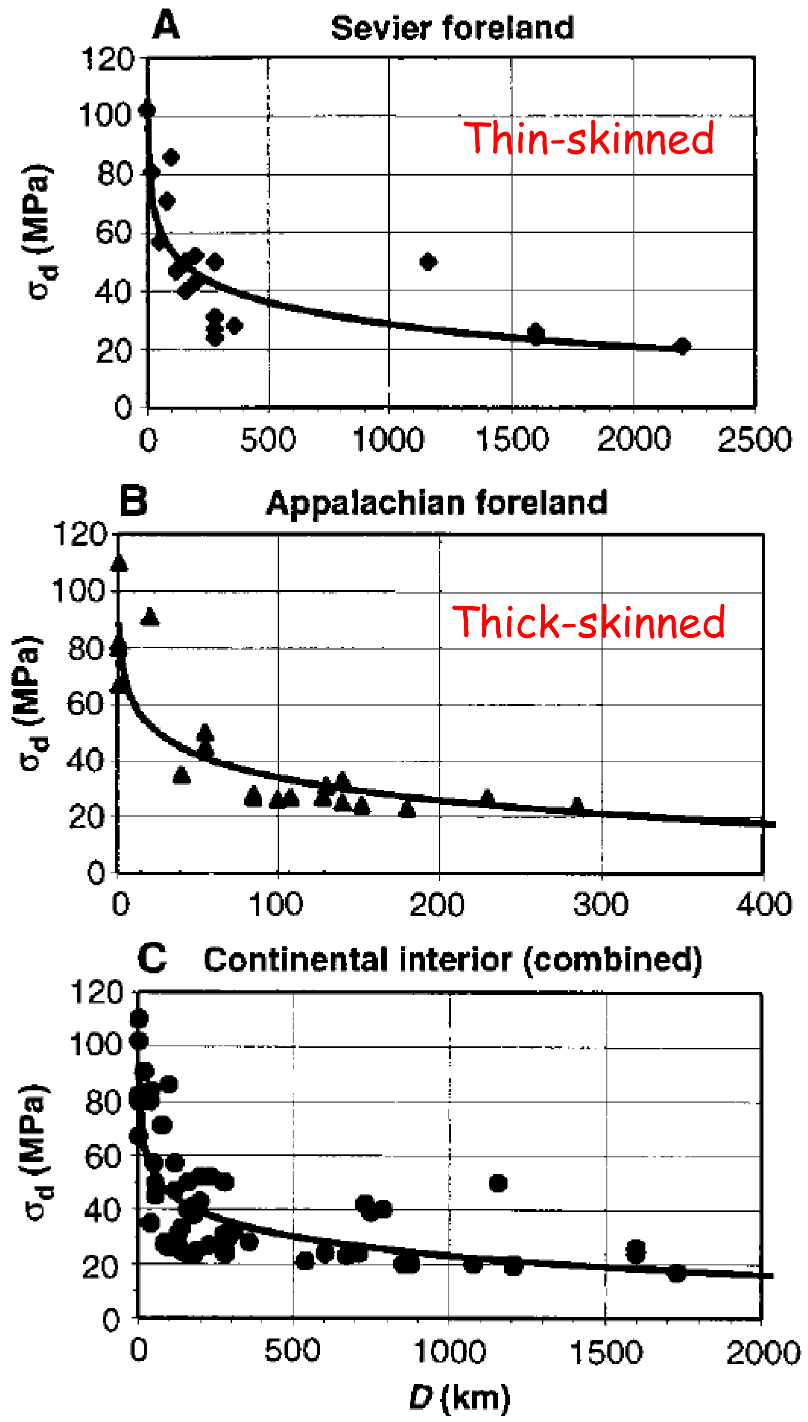

Is stress transmission really independent on structural style of orogens as claimed ?

Issue : no normalization to depth

Q2 : How does deformation distribute and propagate during thick-skinned tectonics ?
Is the sequence of deformation the same than for thin-skinned style ?

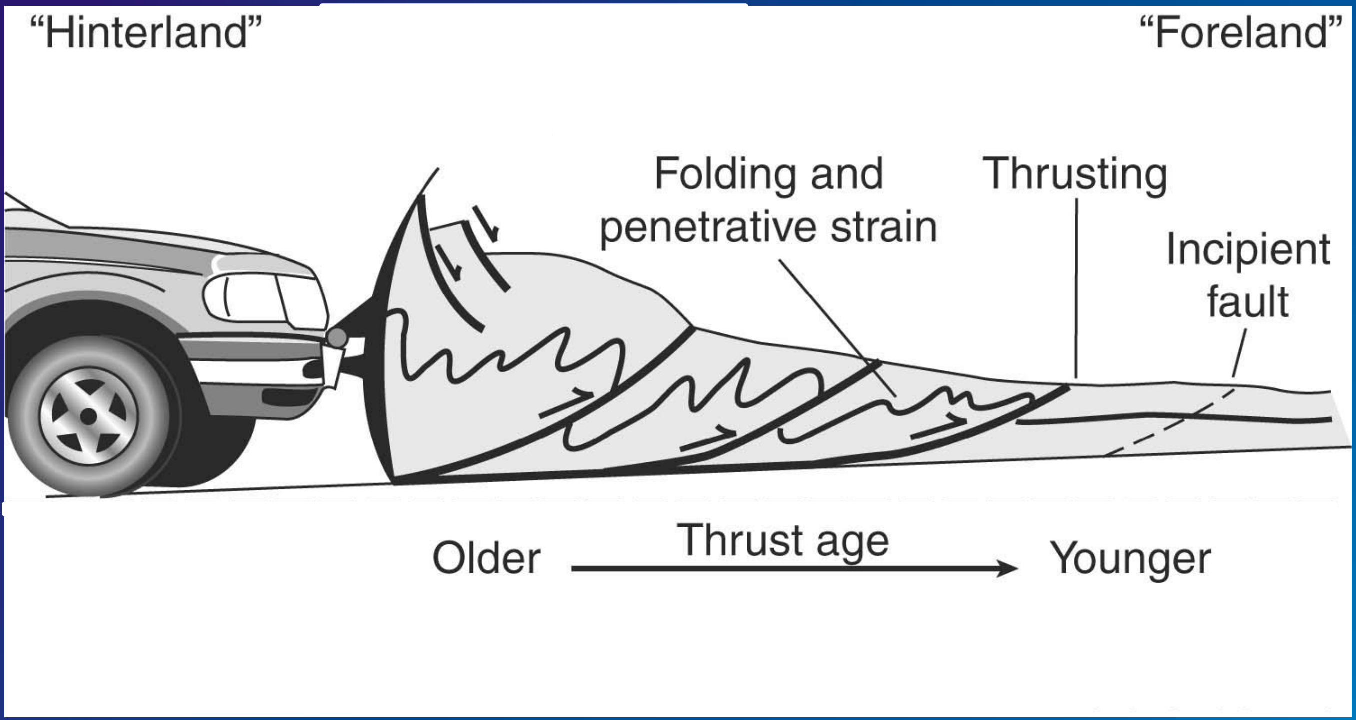

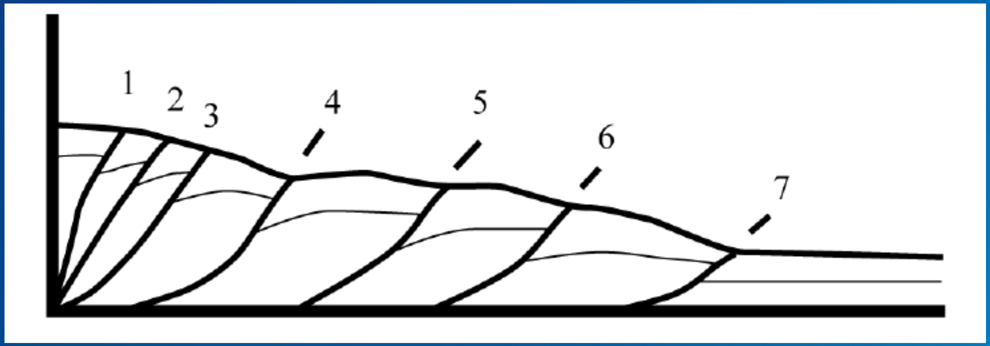

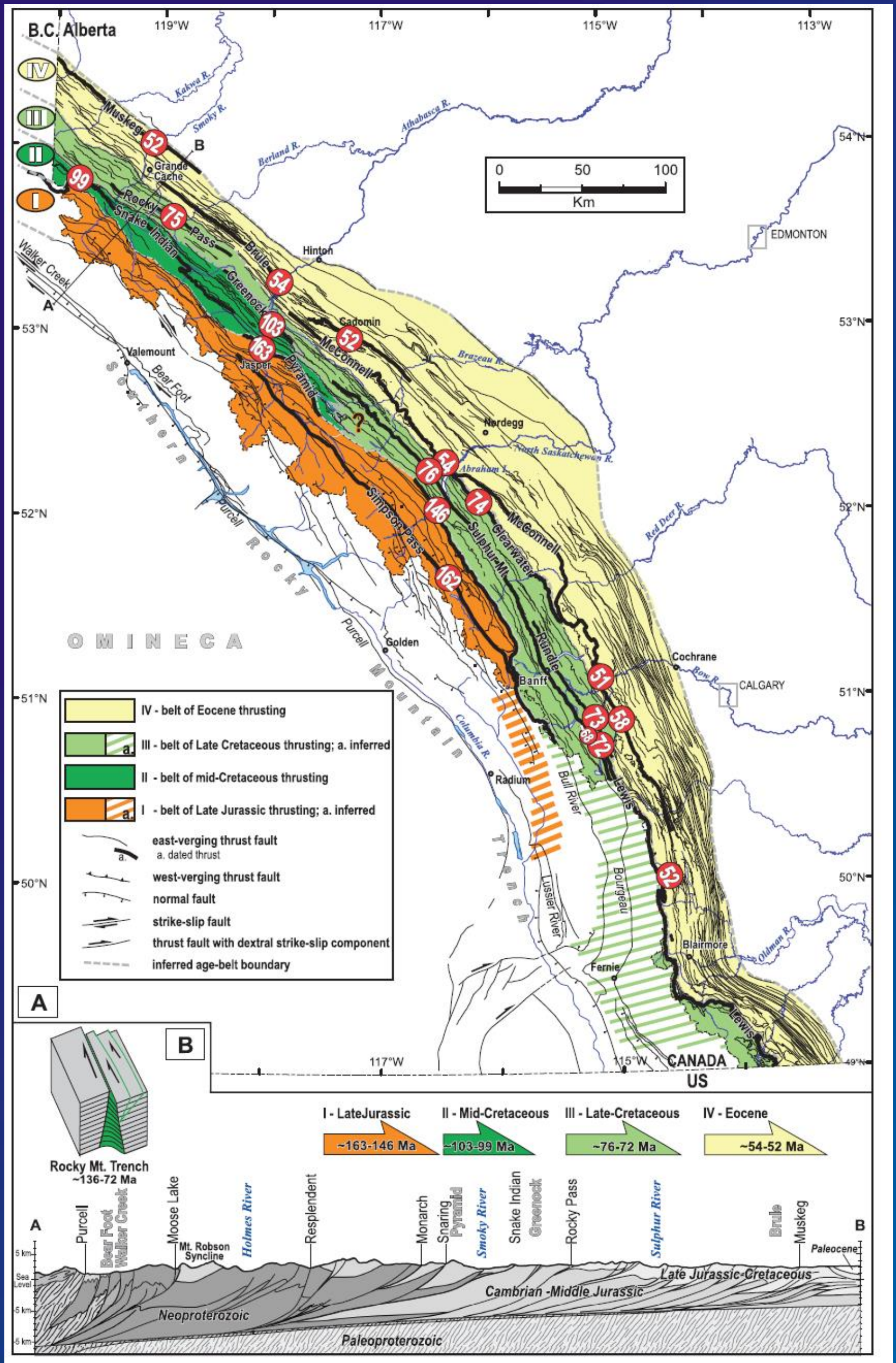

(Pana and Van der Pluijm, 2015)

Evidence for orogenic pulses and outward sequence of Sevier deformation in the thin-skinned Alberta Rocky Mountains
by 40Ar/39Ar dating of illites from
gouges of major fault zones

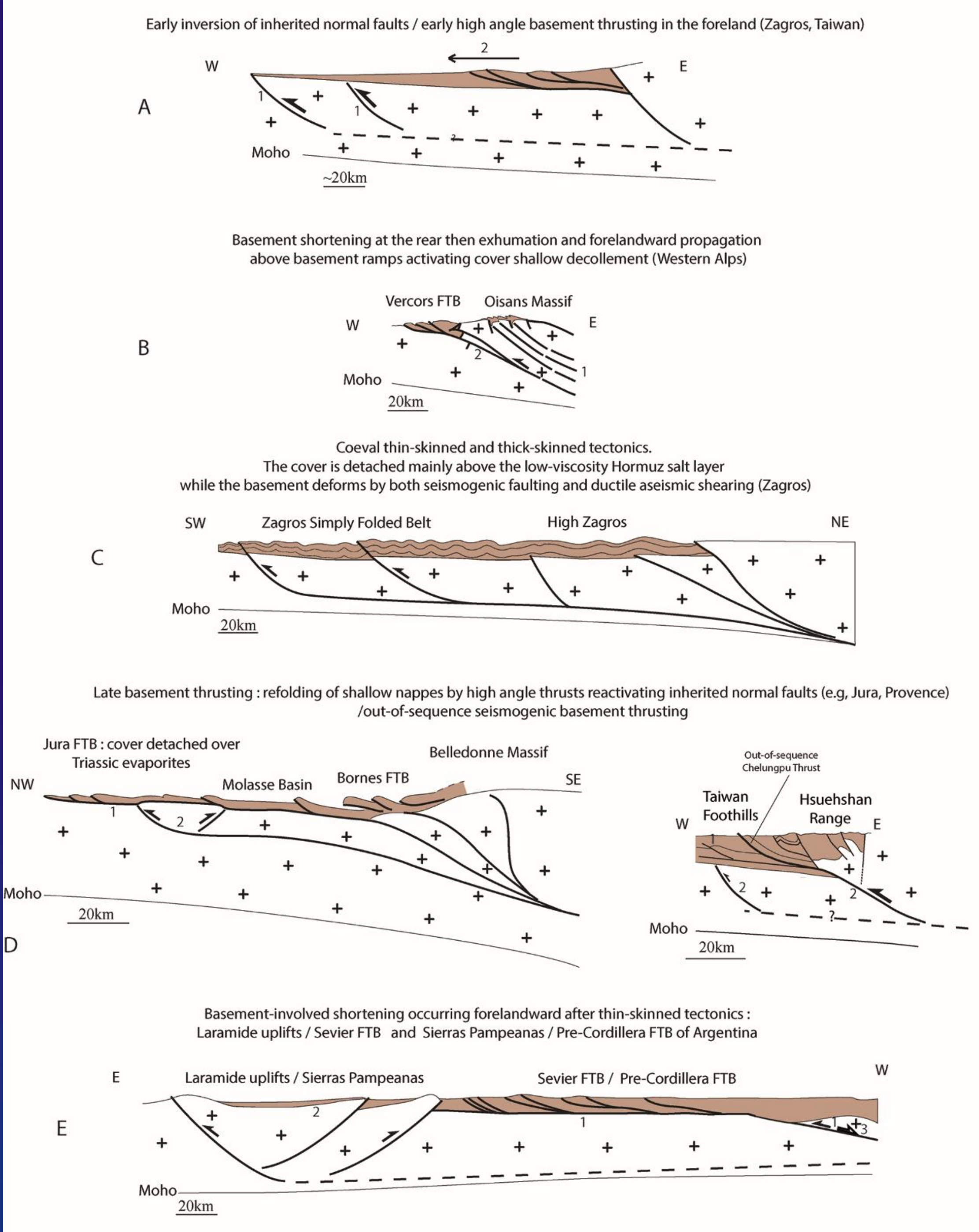

Sequence of thick-skinned versus thin-skinned tectonics in FTBs

(Lacombe and Bellahsen, 2016)

Thick-skinned tectonics :

Expected more erratic sequence due to inherited faults with variable orientation and strength ?

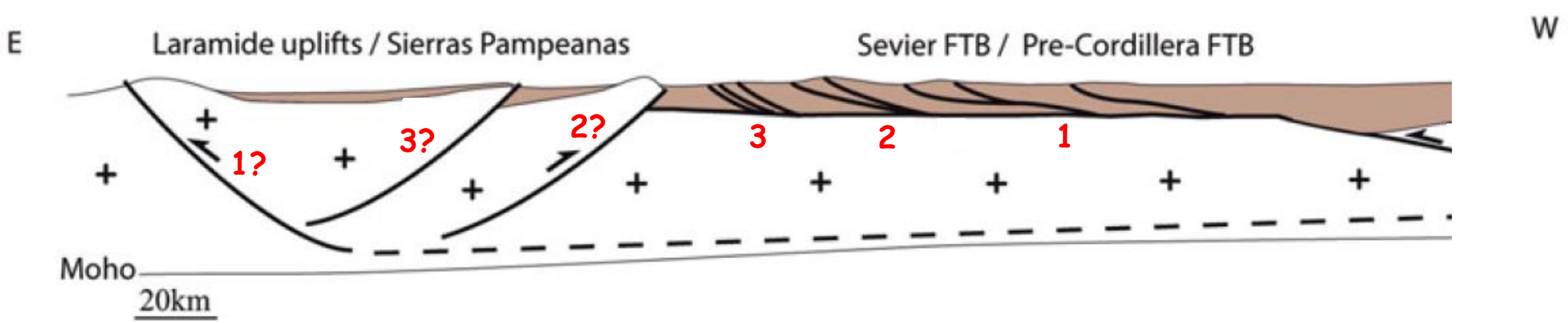


WELCOME TO
WYOMING
FOREVER WEST

Long-lasting subduction of the Farallon plate along the North America margin

The Sevier belt formed and propagated eastward as a thin-skinned wedge during Cretaceous to early Paleocene times.
Thick-skinned Laramide deformation initiated cratonwards by Late Cretaceous until Paleogene times
→ time overlap with final stages of Sevier deformation.

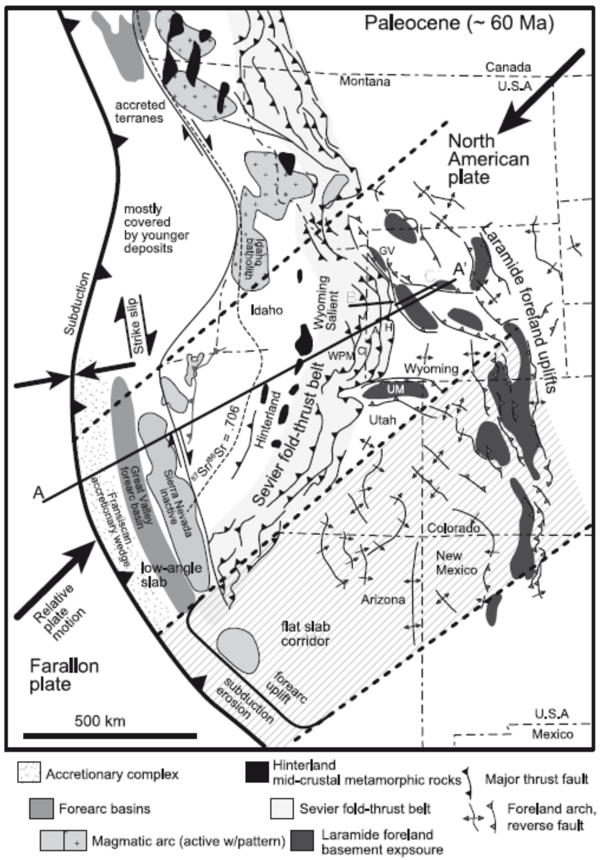

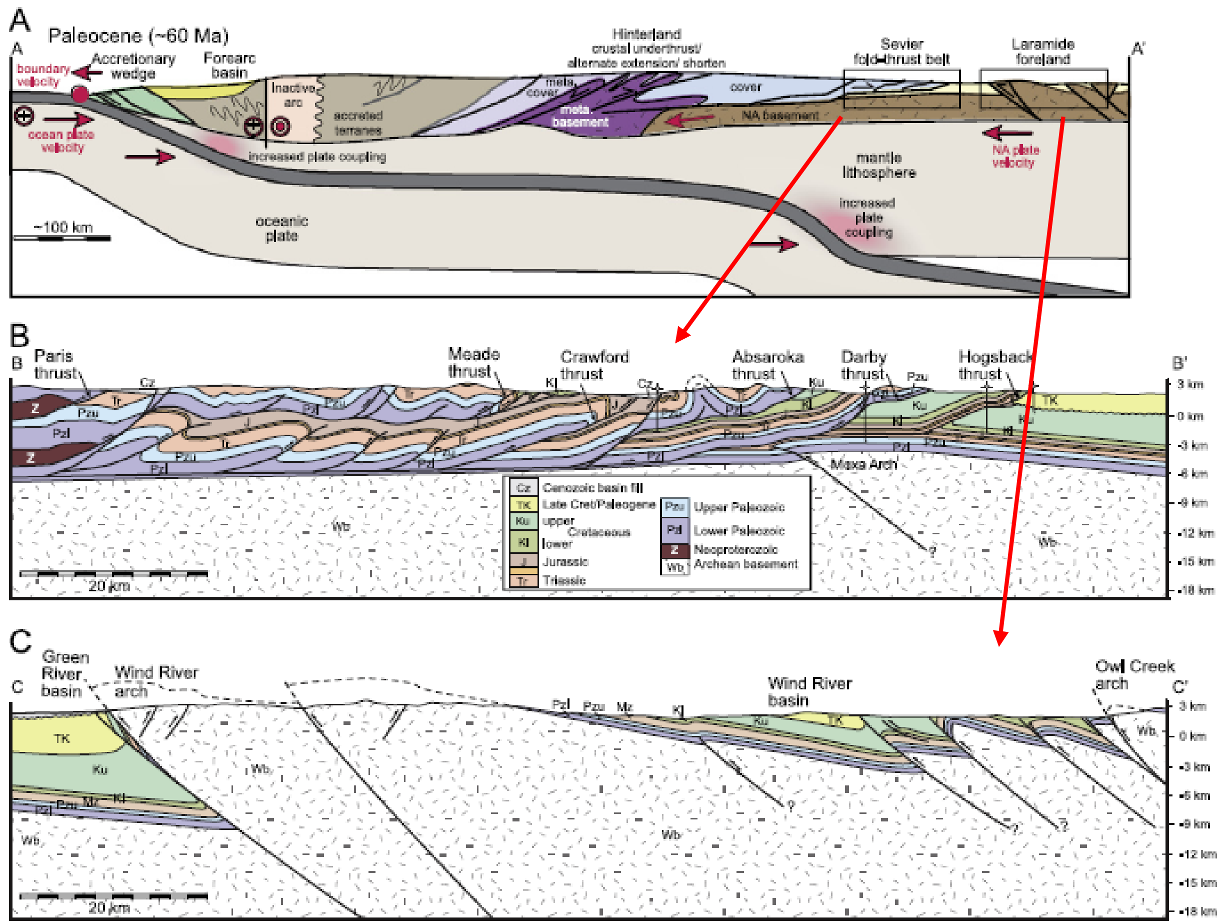

(Weil and Yonkee, 2012)

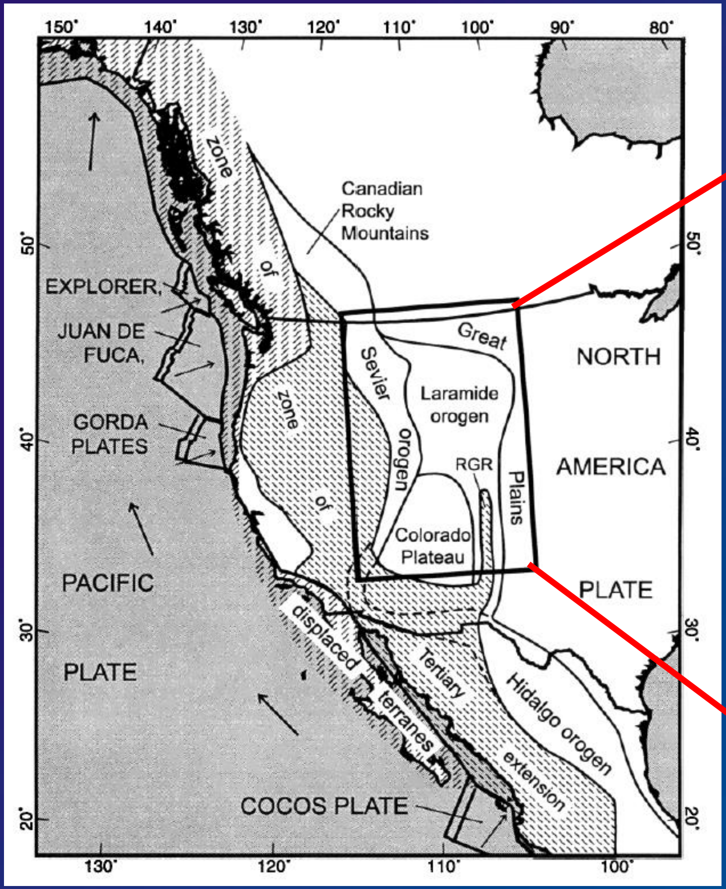

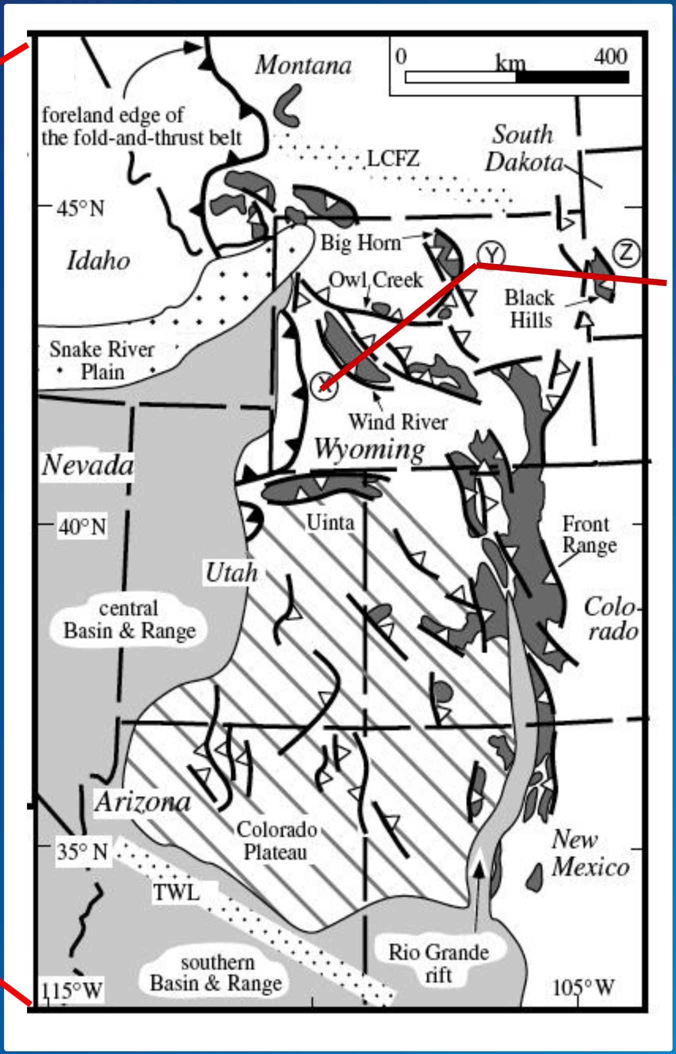

(Marshak et al., 2000; Lacombe and Bellahsen, 2016)

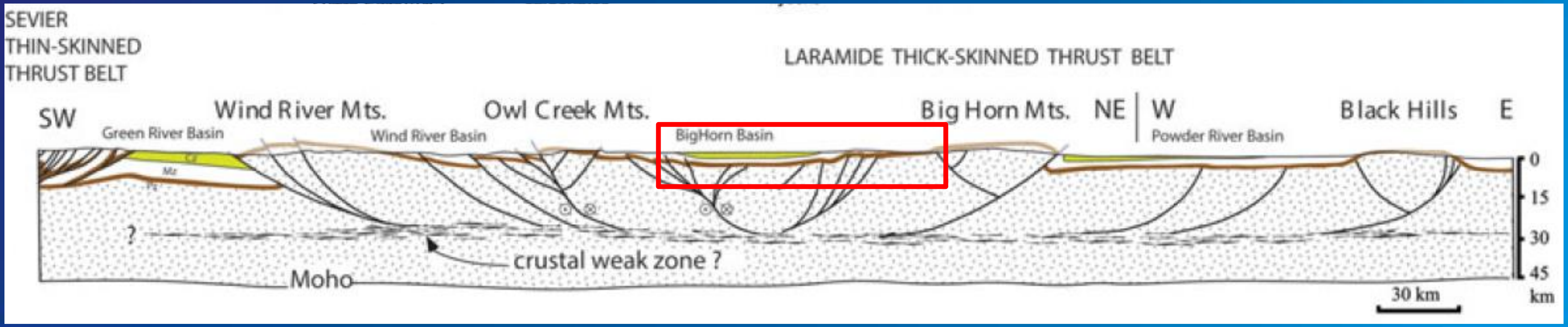

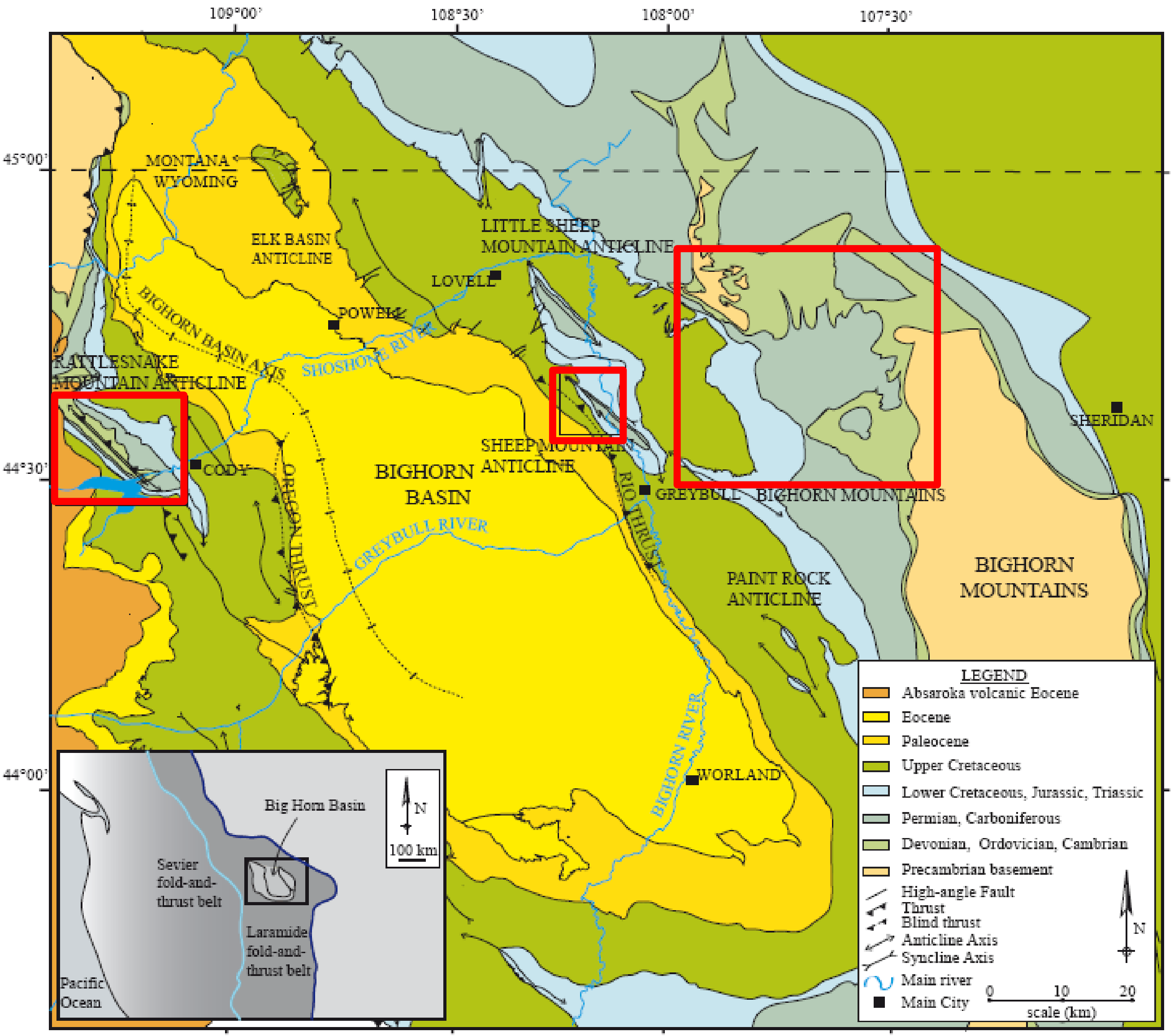

109°00'
108°30'
108°00'
107°30'
45°00'
44°30'
44°00'
MONTANA
WYOMING
ELK BASIN ANTICLINE
LITTLE SHEEP MOUNTAIN ANTICLINE
LOVELL
POWELL
BIGHORN BASIN AXIS
SHOSHONE RIVER
RATTLESNAKE MOUNTAIN ANTICLINE
CODY
OREGON THRUST
BIGHORN BASIN
SHEEP MOUNTAIN ANTICLINE
RIO THRUST
GREYBULL
BIGHORN MOUNTAINS
SHERIDAN
GREYBULL RIVER
PAINT ROCK ANTICLINE
BIGHORN MOUNTAINS
BIGHORN RIVER
WORLAND
Big Horn Basin
Sevier fold-and-thrust belt
Laramide fold-and-thrust belt
Pacific Ocean
N
100 km
LEGEND
Absaroka volcanic Eocene
Eocene
Paleocene
Upper Cretaceous
Lower Cretaceous, Jurassic, Triassic
Permian, Carboniferous
Devonian, Ordovician, Cambrian
Precambrian basement
High-angle Fault
Thrust
Blind thrust
Anticline Axis
Syncline Axis
Main river
Main City
N
0 10 20
scale (km)

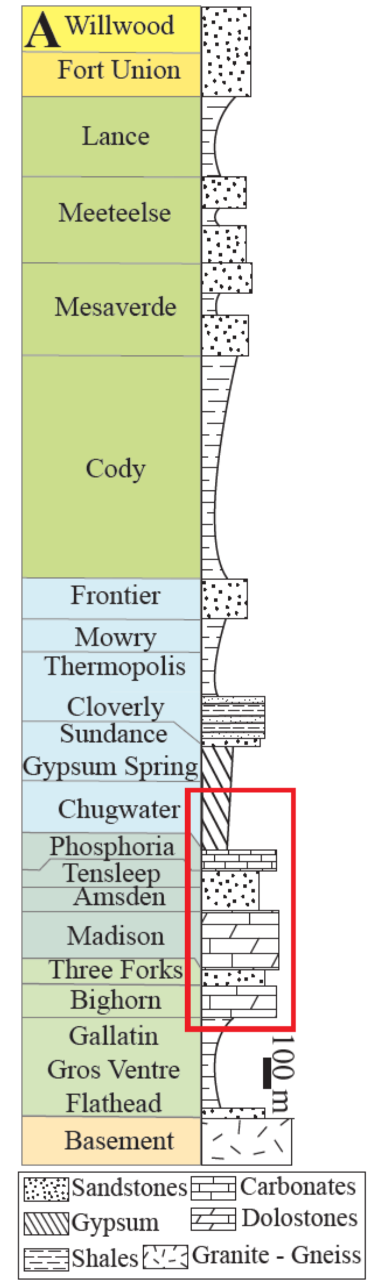

A
Willwood
Fort Union
Lance
Meeteelse
Mesaverde
Cody
Frontier
Mowry
Thermopolis
Cloverly
Sundance
Gypsum Spring
Chugwater
Phosphoria
Tensleep
Amsden
Madison
Three Forks
Bighorn
Gallatin
Gros Ventre
Flathead
Basement
100 m
Sandstones
Carbonates
Gypsum
Dolostones
Shales
Granite - Gneiss

Western BigHorn Mountains

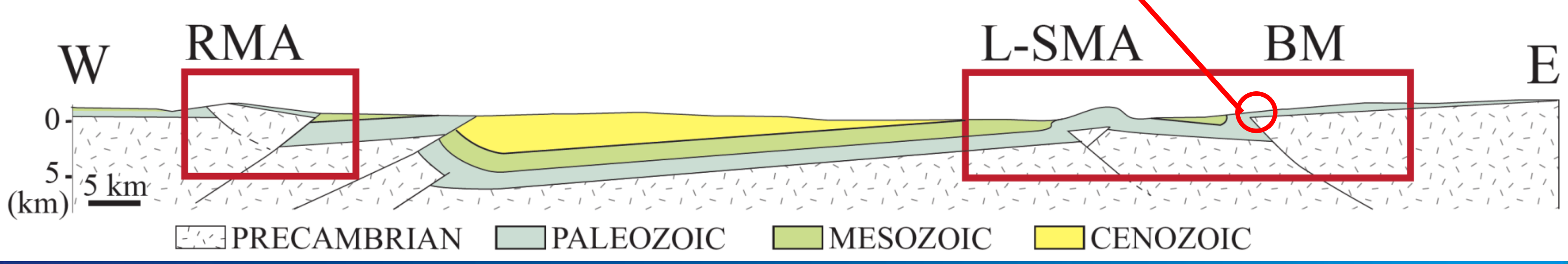

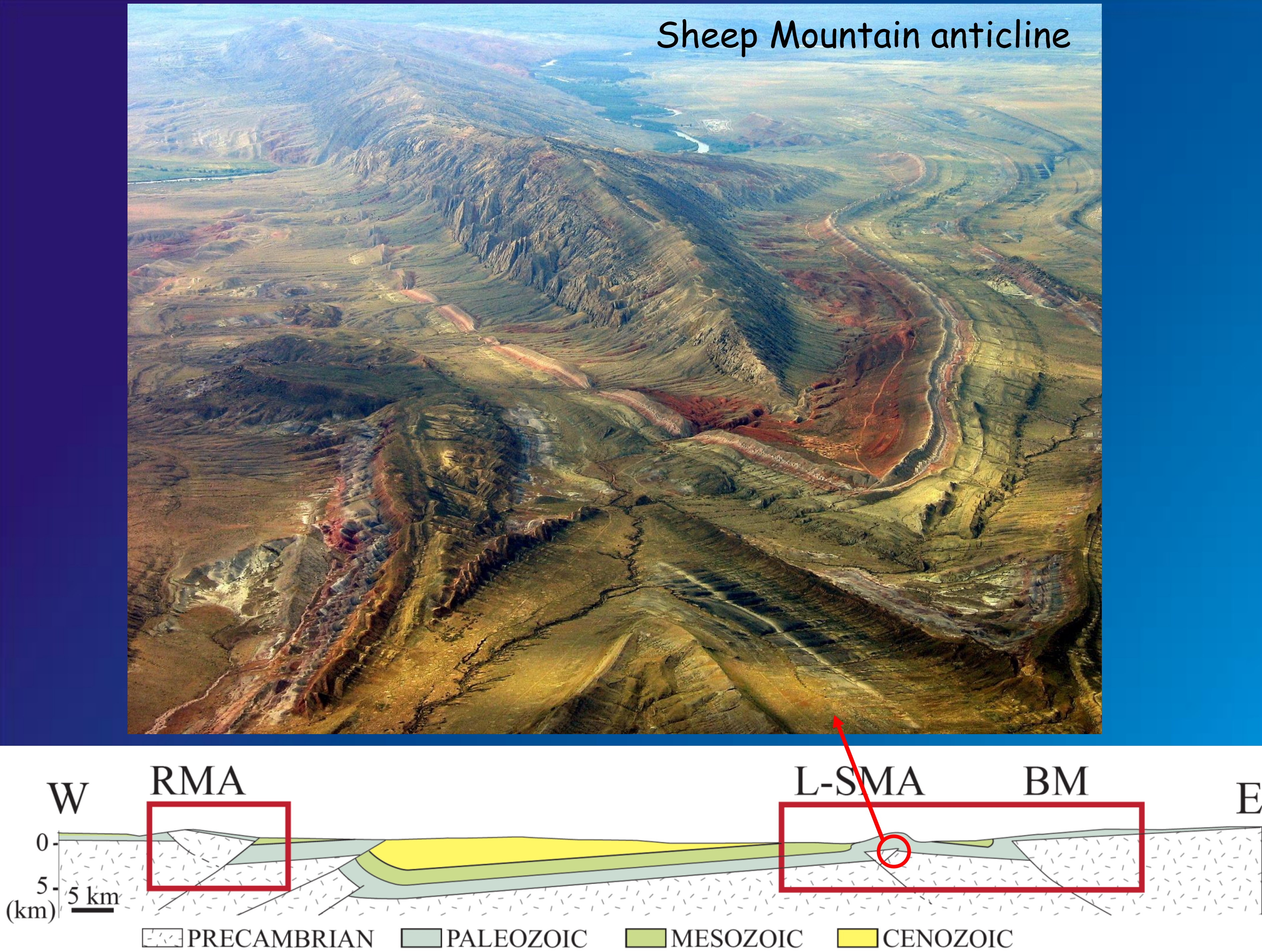
Sheep Mountain anticline
W
RMA
L-SMA
BM
E
0
5
(km)
5 km
PRECAMBRIAN
PALEOZOIC
MESOZOIC
CENOZOIC

Sheep Mountain anticline

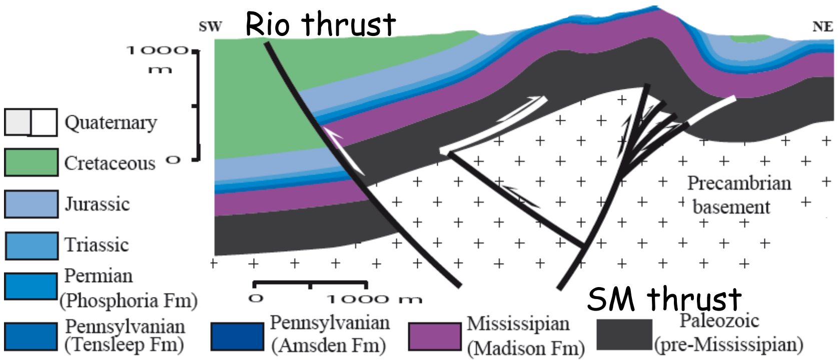

(Amrouch et al., 2010)

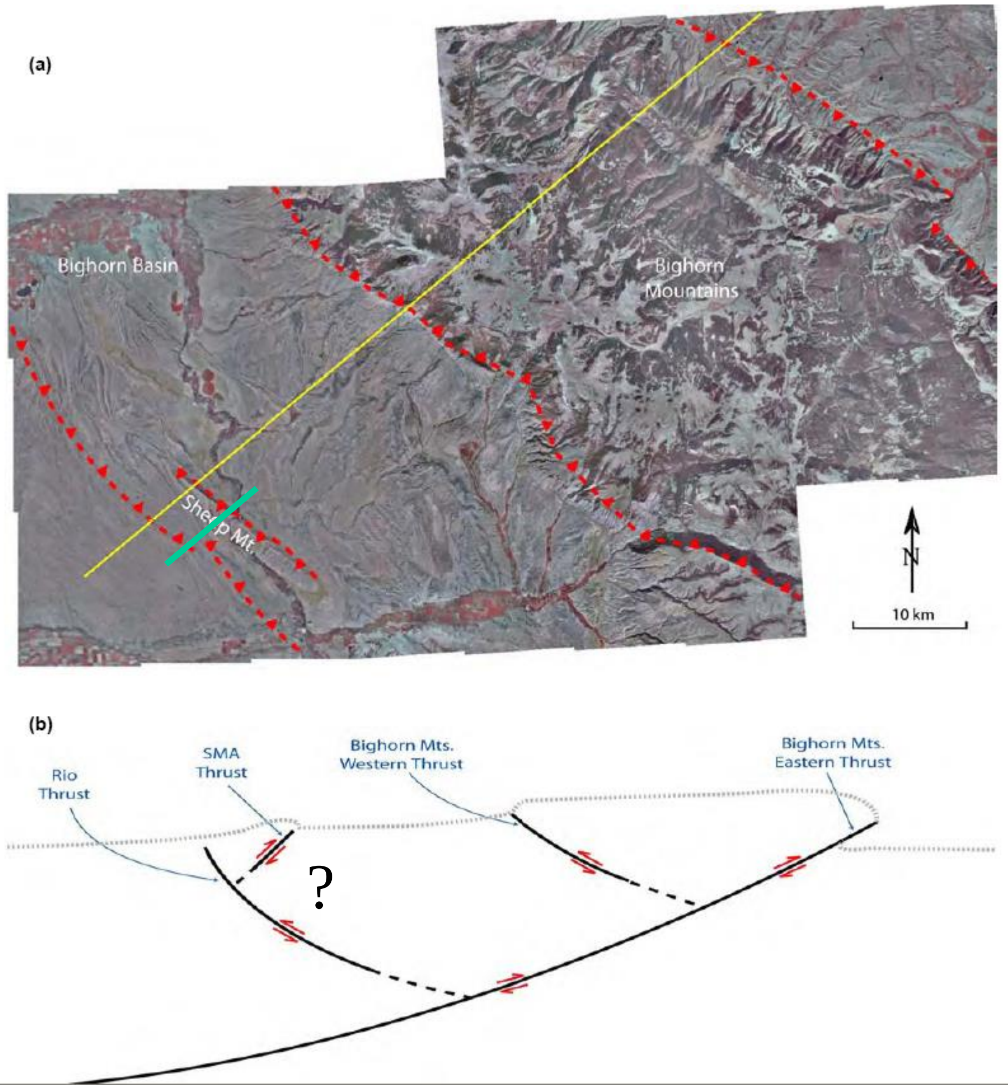

Still debated thrust sequence !

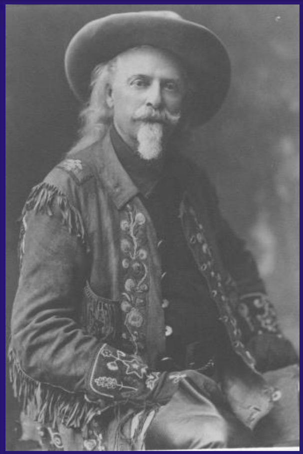


Rattlesnake Mountain anticline
OLD TRAIL TOWN
A Great Family Experience
OPEN
Cody
Cowboy Village
Rated #1 Hotel by Tripadvisor.com

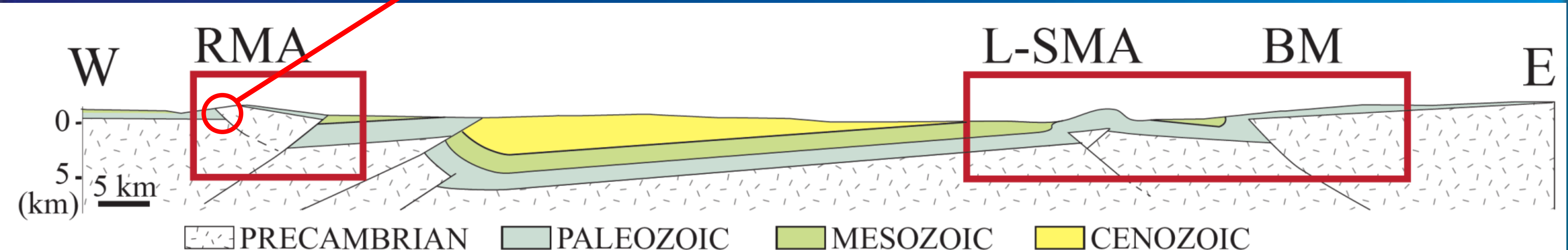
W
RMA
L-SMA
BM
E
0
5
(km)
5 km
PRECAMBRIAN
PALEOZOIC
MESOZOIC
CENOZOIC

Rattlesnake Mountain anticline

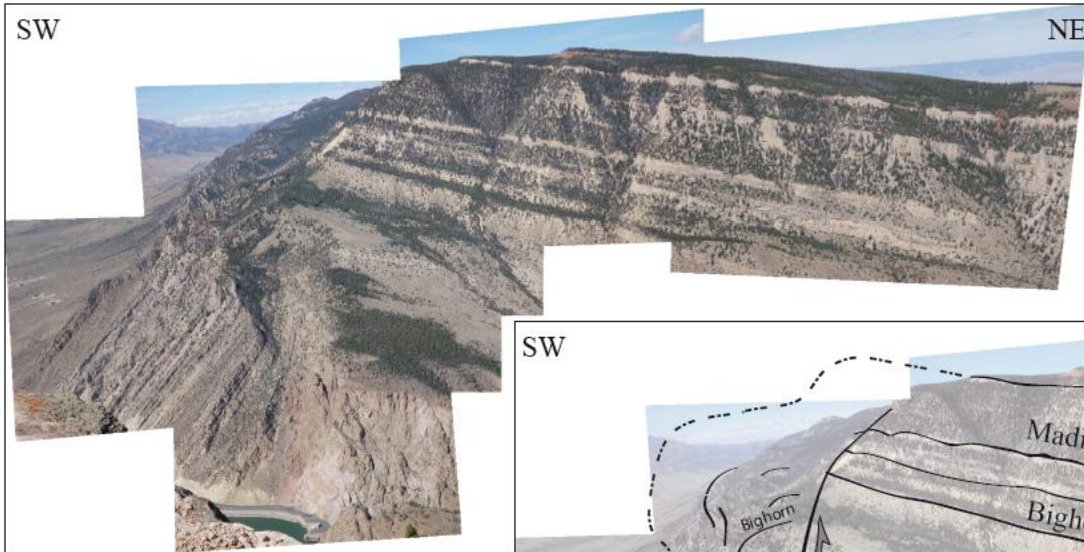

(Beaudoin et al., 2012)

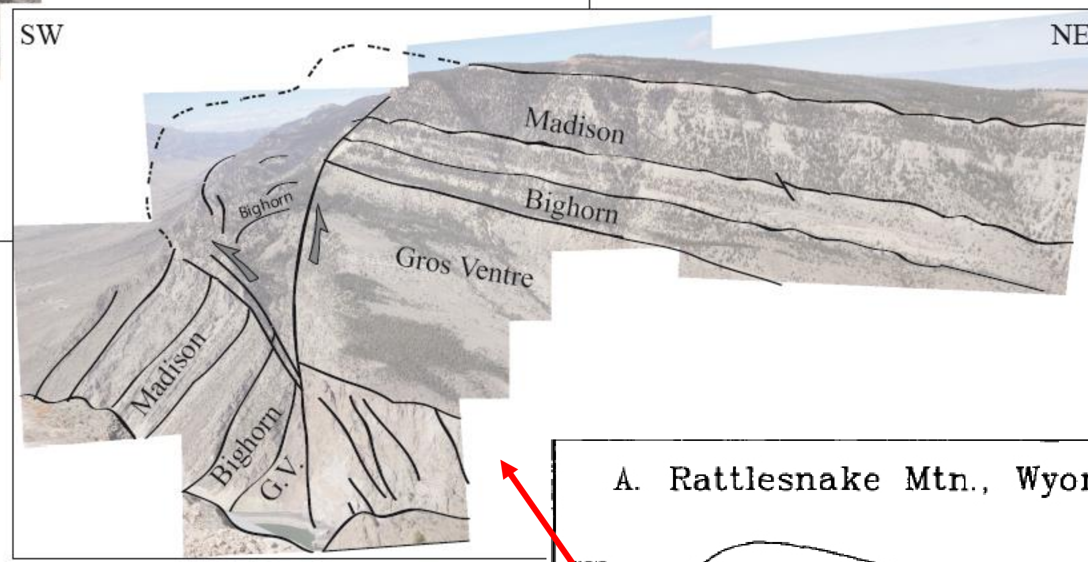

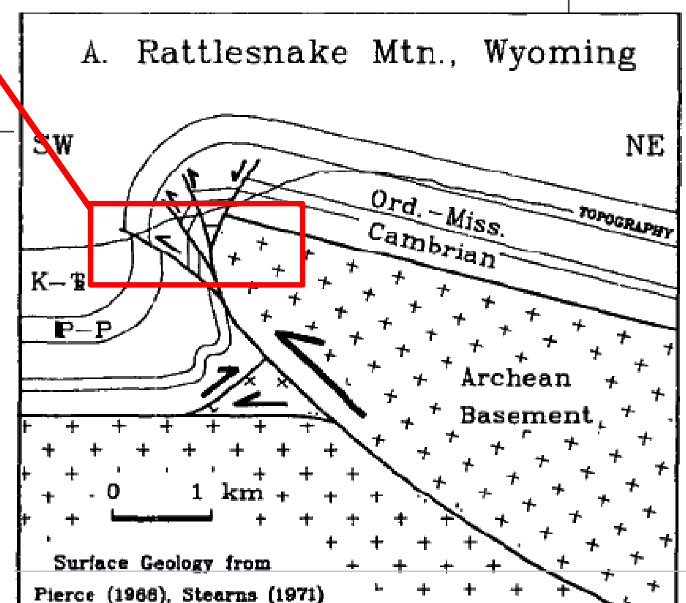

(Erslev, 1986)

Sheep Mountain anticline

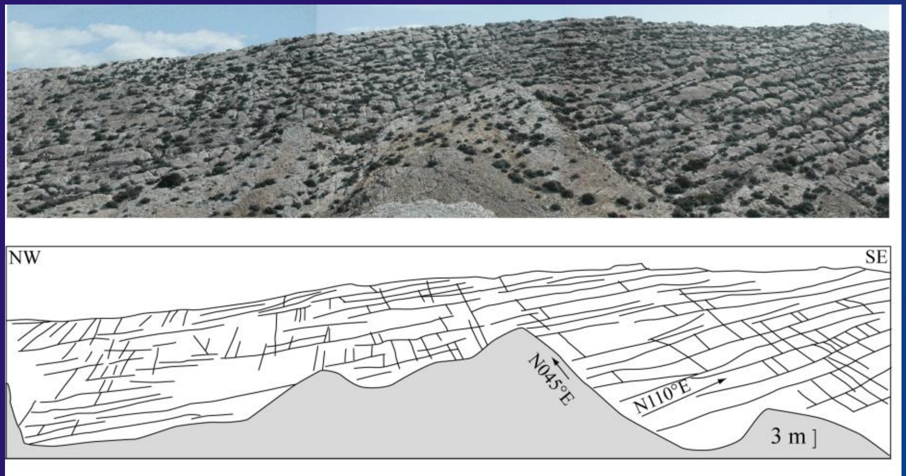

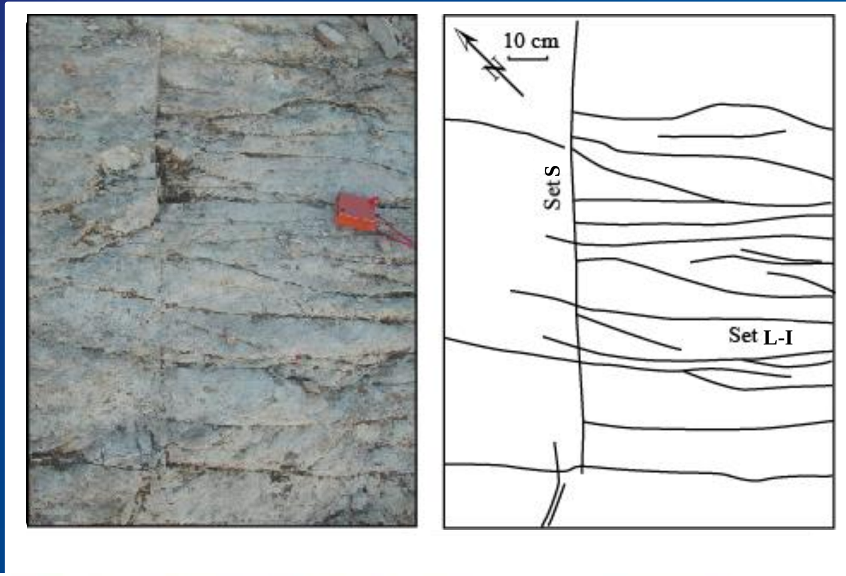

(Bellahsen et al., 2006; Amrouch et al., 2010; Beaudoin et al., 2012)

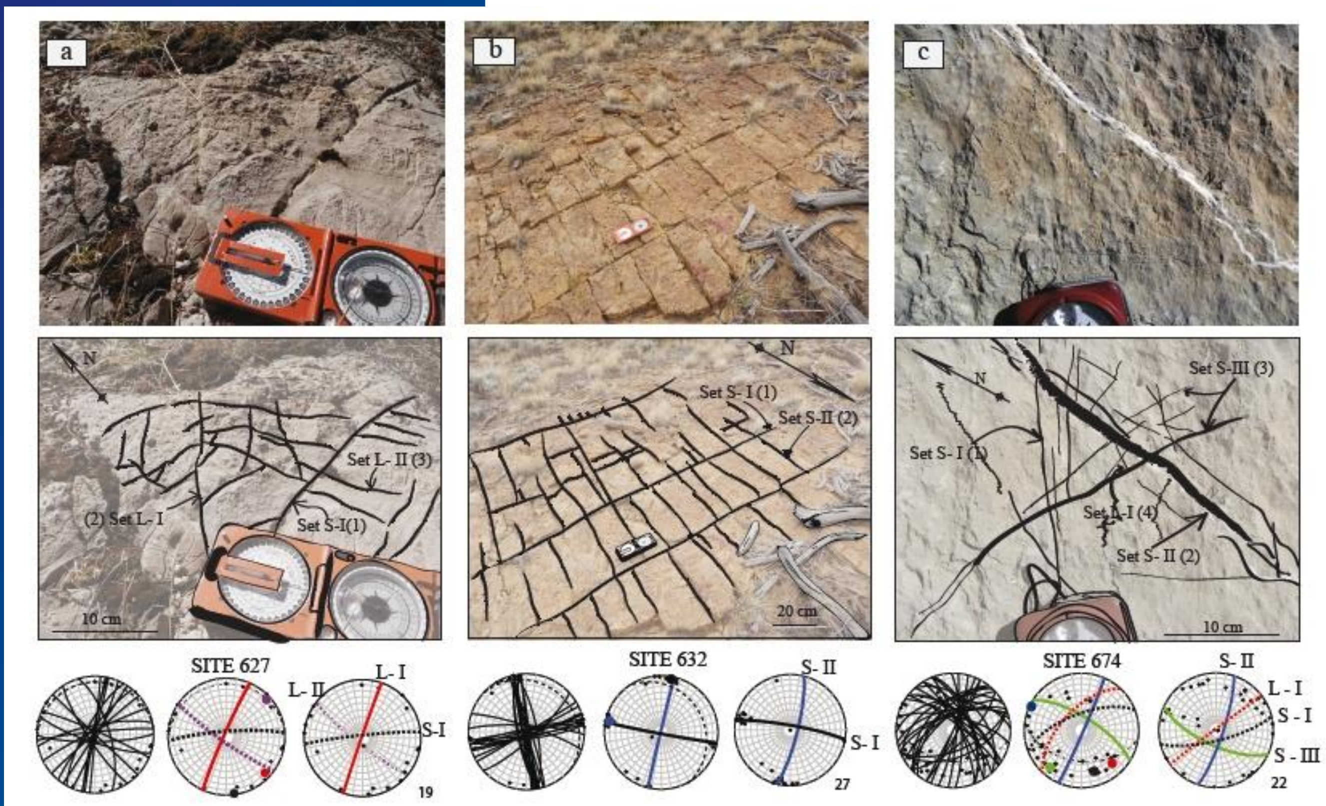

Rattlesnake Mountain anticline

Pressure-solution and meso-scale faulting at Sheep Mountain anticline

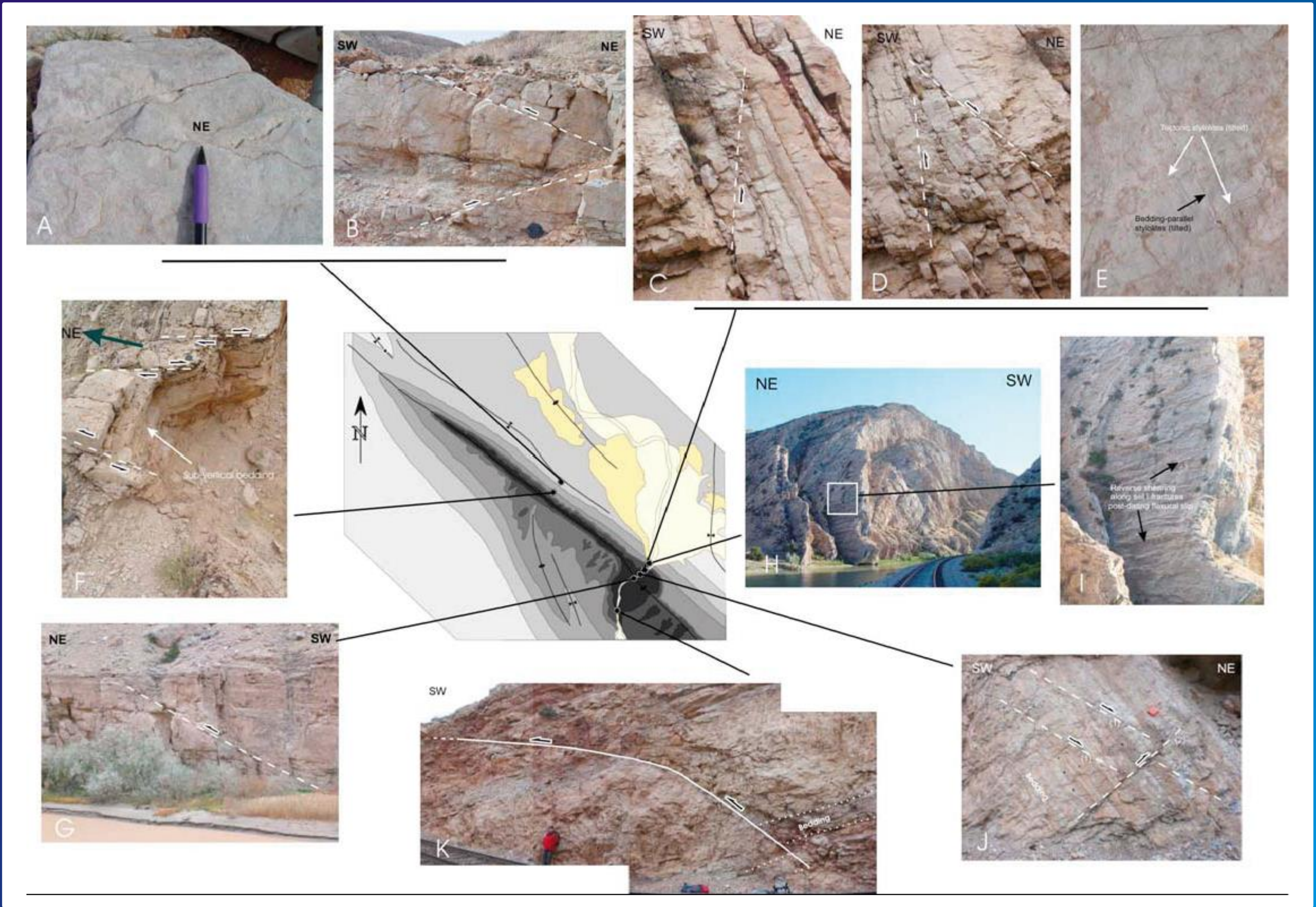

(Amrouch et al., 2010)

Sequence of fault-vein development at Sheep Mountain anticline

(Amrouch et al., 2011)

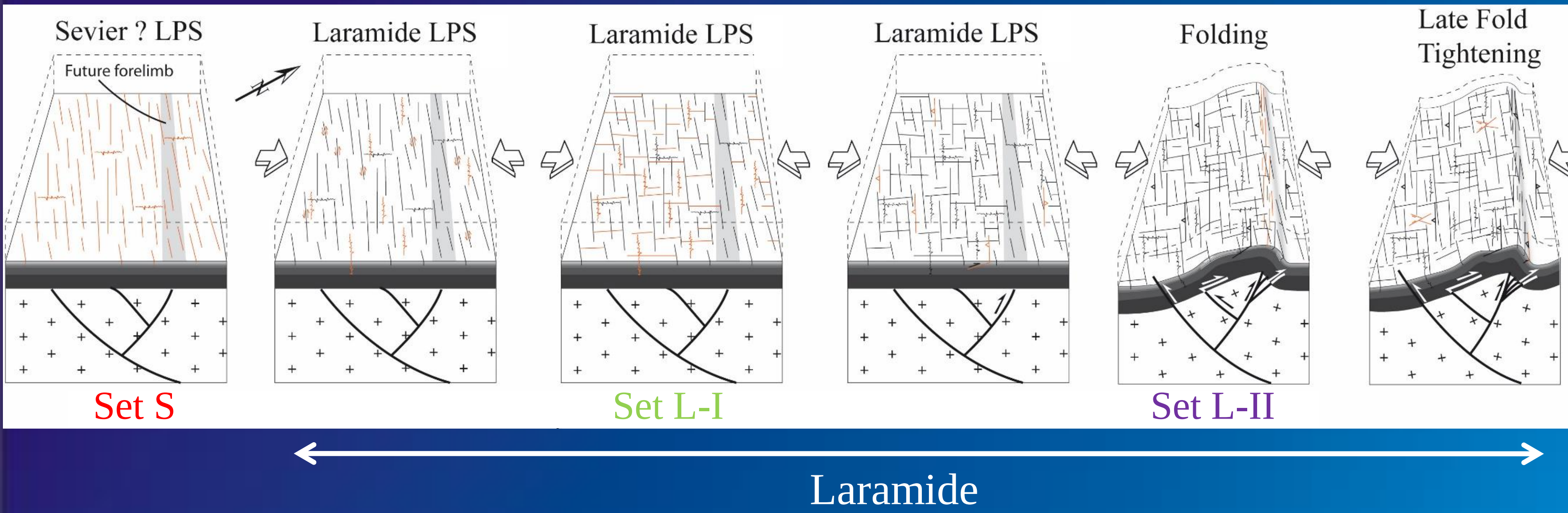

- Mode I opening of pre-Laramide set S joints/veins
- Shear reactivation of pre-Laramide set S veins (LPS).
- Laramide stylolites with NE-trending peaks and mode I opening of set L-I veins (LPS)
- Reverse faulting parallel to the fold axis (LPS).
- Mode I opening of syn-folding, outer-rim extension-related set L-II veins
- Late stage fold tightening (LSFT) marked by strike-slip faults and reactivation of tilted set S joints/veins as small reverse faults in the forelimb

Fracture set	Mean strike of fractures	Paleostress from fractures	Paleostress from striated microfaults	Paleostress from calcite twins	Related Tectonic events
Set S-I	090°E to 060°E	σ_3 σ_1 ?			Sevier layer-parallel shortening ?
Set S-II	180°E to 020°E	σ_3			Formation of the flexural foreland basin
Set S-III	110°E	σ_3 σ_1 ?	σ_1	σ_1	Sevier layer-parallel shortening ?
Set L-I	045°E	σ_3 σ_1 ?	σ_3 σ_1	σ_1 σ_3	Laramide layer-parallel shortening
Set L-II	135°E	σ_3		σ_3	Local curvature-related extension
Set L-III	045°E		σ_1	σ_1 σ_3	Late stage fold tightening
Set P-I	180°E to 160°E	σ_3		σ_3	Basin and Range extension

Pre-Laramide
Laramide
Post Laramide

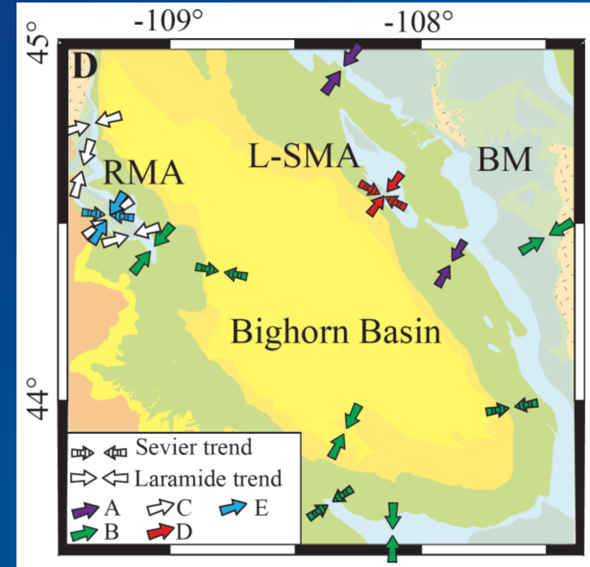

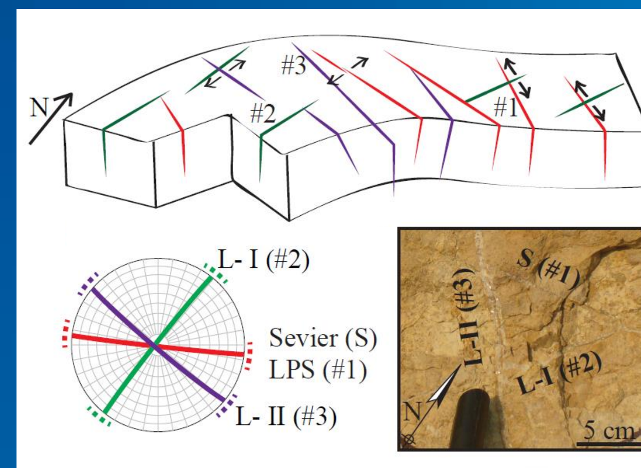

Stress history of the Bighorn Basin = polyphase

Laramide stress + pre-Laramide (Sevier ?) stress + …

Based only on (1) orientations of microstructures and (2) relative chronology between microstuctures and with respect to folding

Direct time constraints ?

In northern Wyoming – Montana, thermochronology and stratigraphy seemingly support an eastward sequence of Laramide deformation

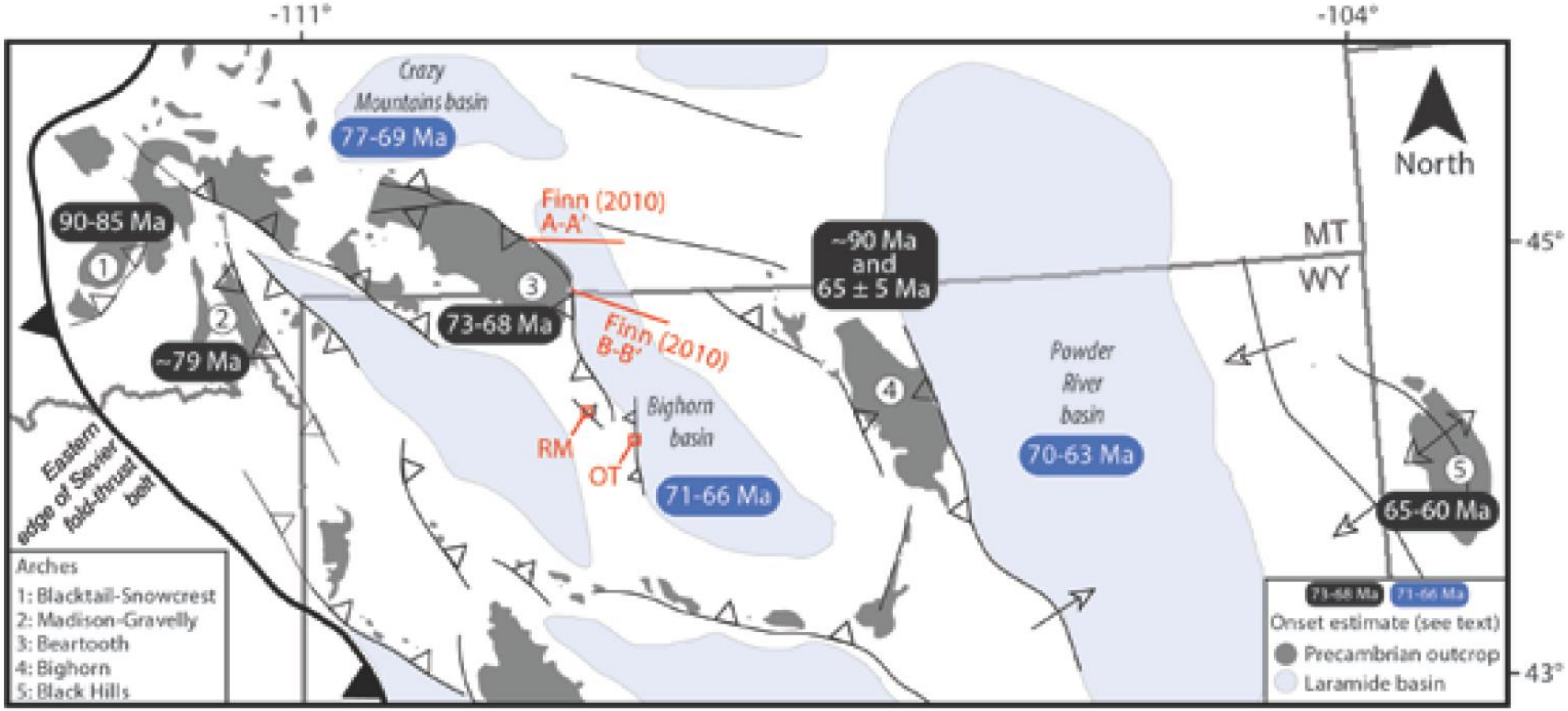

Figure 1. Map showing structural arches and basins discussed herein. RM—Rattlesnake Mountain anticline; OT—Oregon thrust.

(Tacker and Karlstrom, in press))

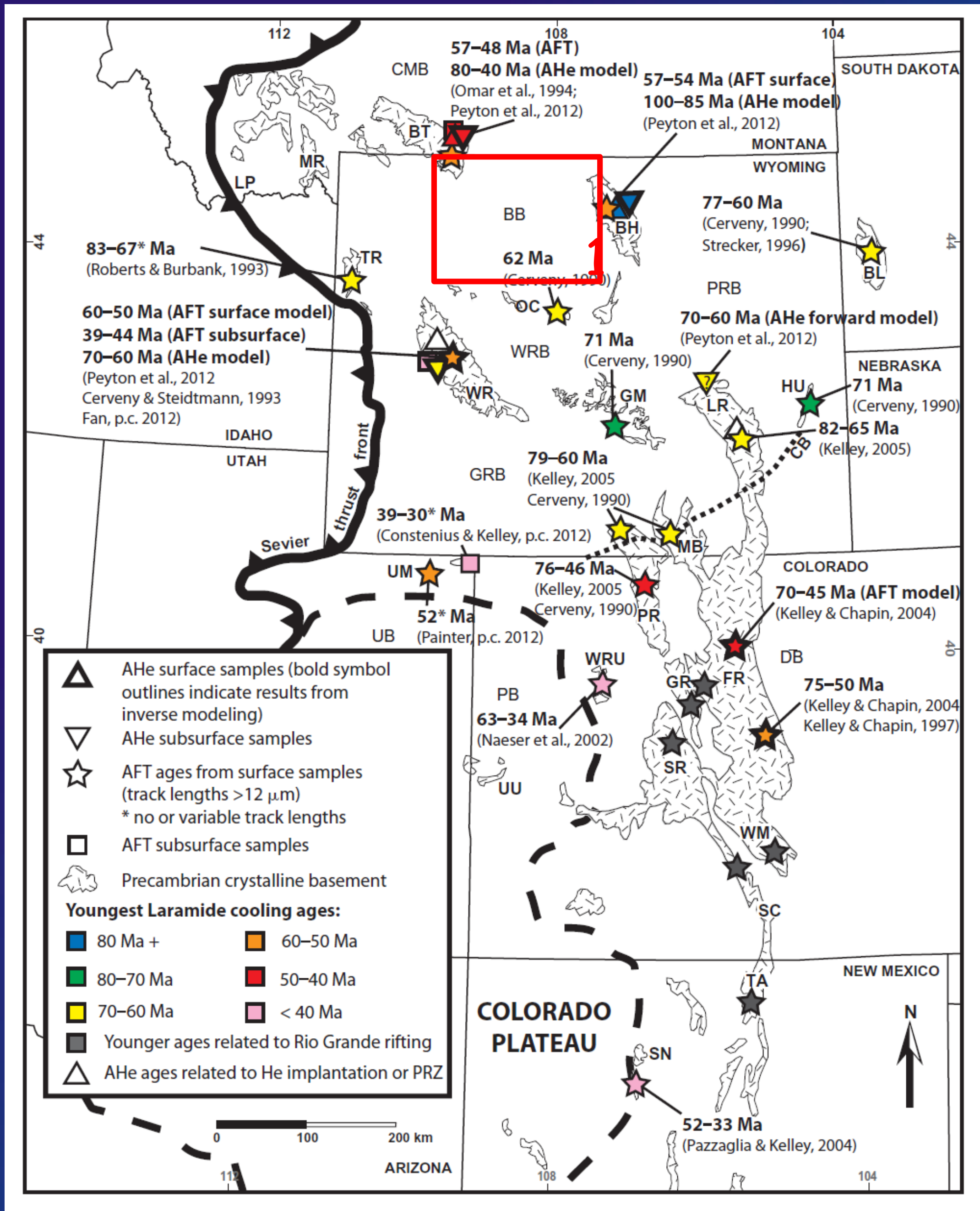

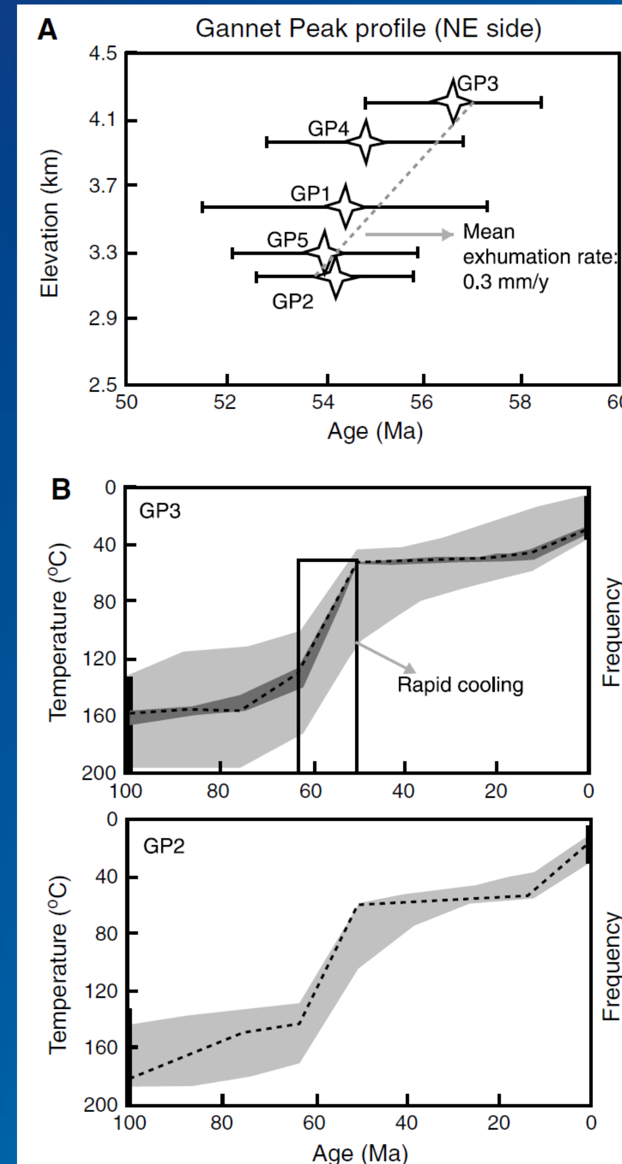

Peyton et al., 2012
Wind River, AFTSolve

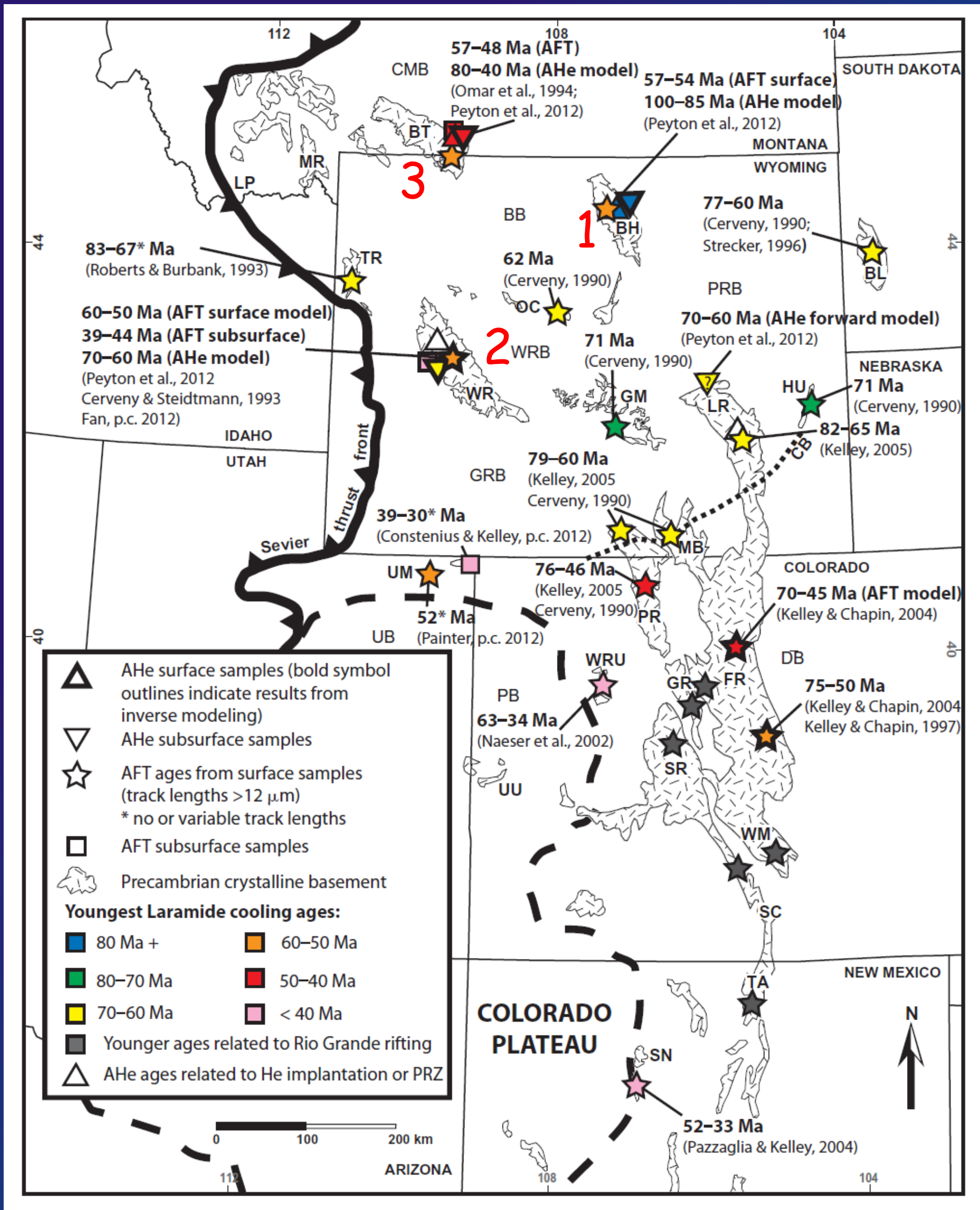

Arches around BHB cooled/exhumed rapidly in a rather westward sequence

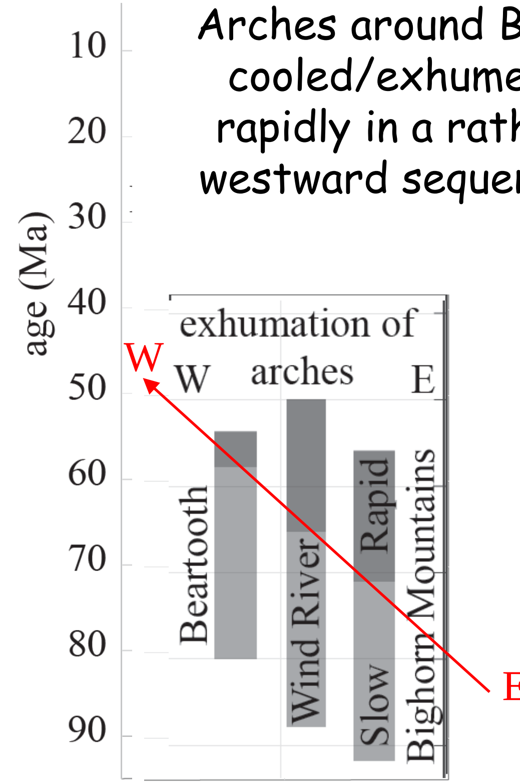

-Bighorn Mountains (91-57 Ma, rapid phase since 71 Ma)
-Wind River Range (90 – 50 Ma, rapid phase since 64 Ma)
- Beartooth Mountains (80-54 Ma, rapid phase since 57 Ma).

TERA-WASSERBURG DIAGRAM

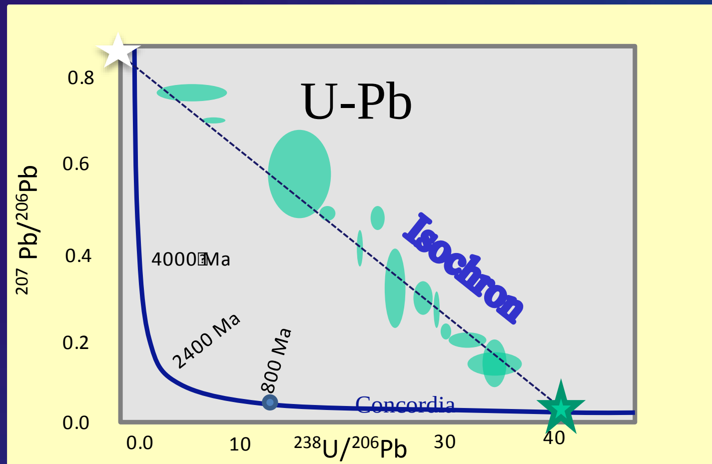

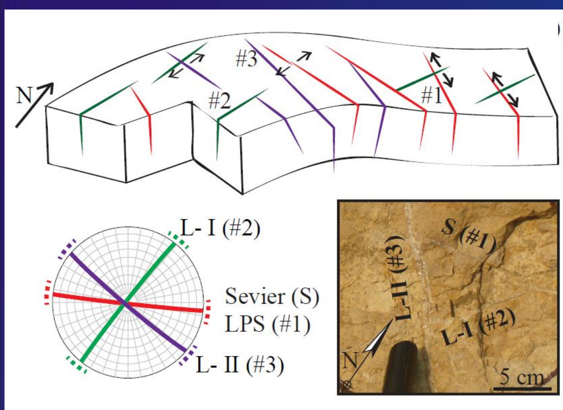

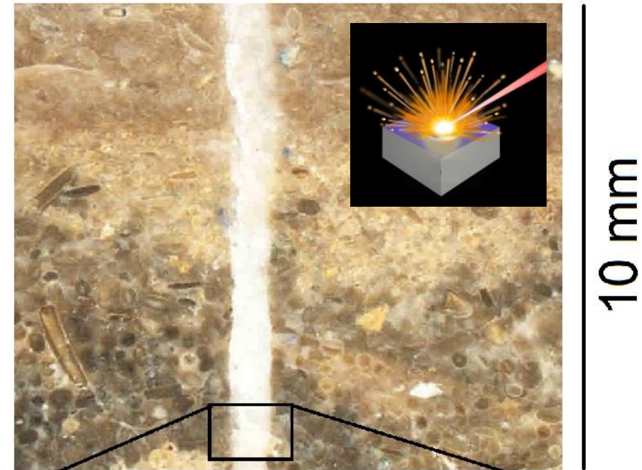

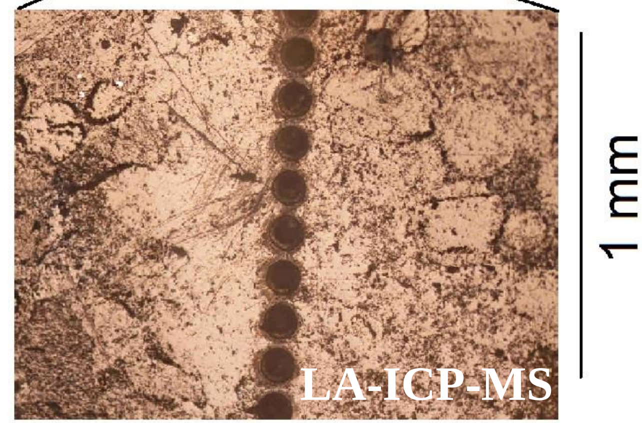

Technically challenging because of low U concentrations (<10 ppm) in calcite
→ several laser spots are needed

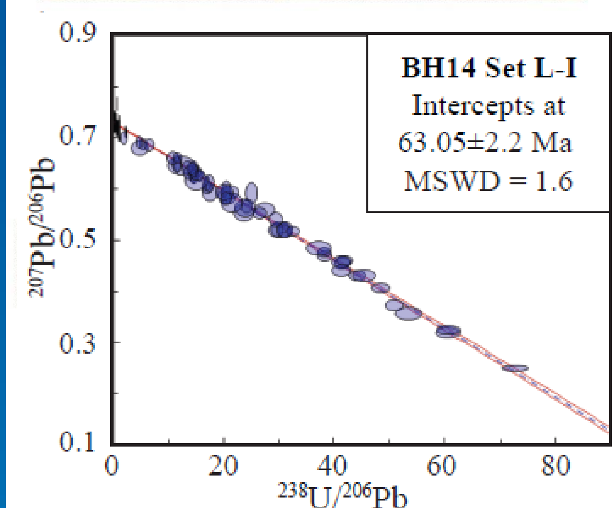

Better if :

- High heterogeneity in U/Pb and Pb/Pb ratios
- High U/Pb
- No mixing among phases
  (eg. partial dolomitization)

Criteria for reliable/accurate ages

1) MSWD < 2.5
Mean Squared Weighted Deviates

2) n > 10 Number of ablation spots

3) Er <5% Relative error

Data acquisition and treatment, Nick Roberts, BGS

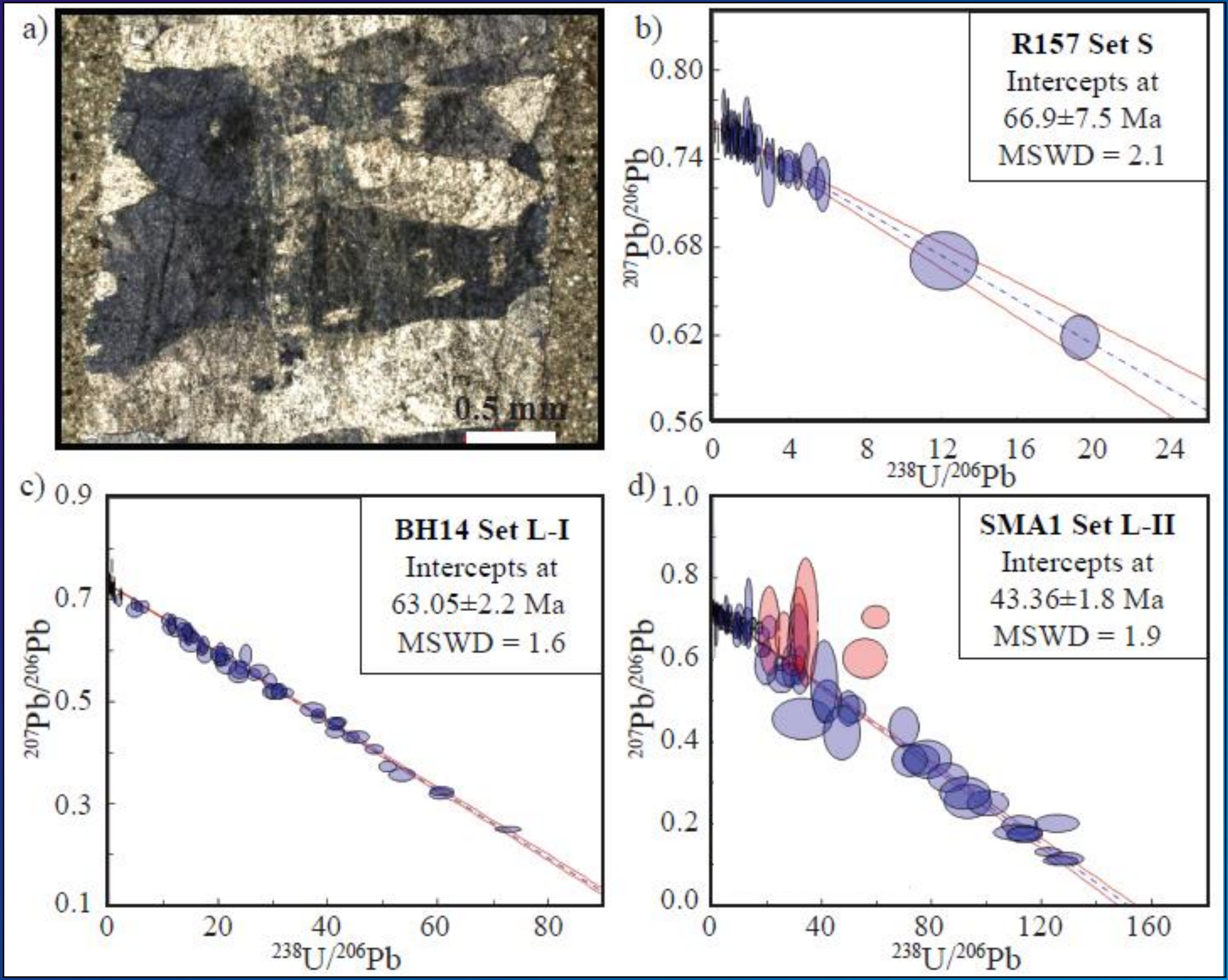

a)
0.5 mm
b)
R157 Set S
Intercepts at
66.9±7.5 Ma
MSWD = 2.1
$^{207}Pb/^{206}Pb$
$^{238}U/^{206}Pb$
c)
BH14 Set L-I
Intercepts at
63.05±2.2 Ma
MSWD = 1.6
$^{207}Pb/^{206}Pb$
$^{238}U/^{206}Pb$
d)
SMA1 Set L-II
Intercepts at
43.36±1.8 Ma
MSWD = 1.9
$^{207}Pb/^{206}Pb$
$^{238}U/^{206}Pb$

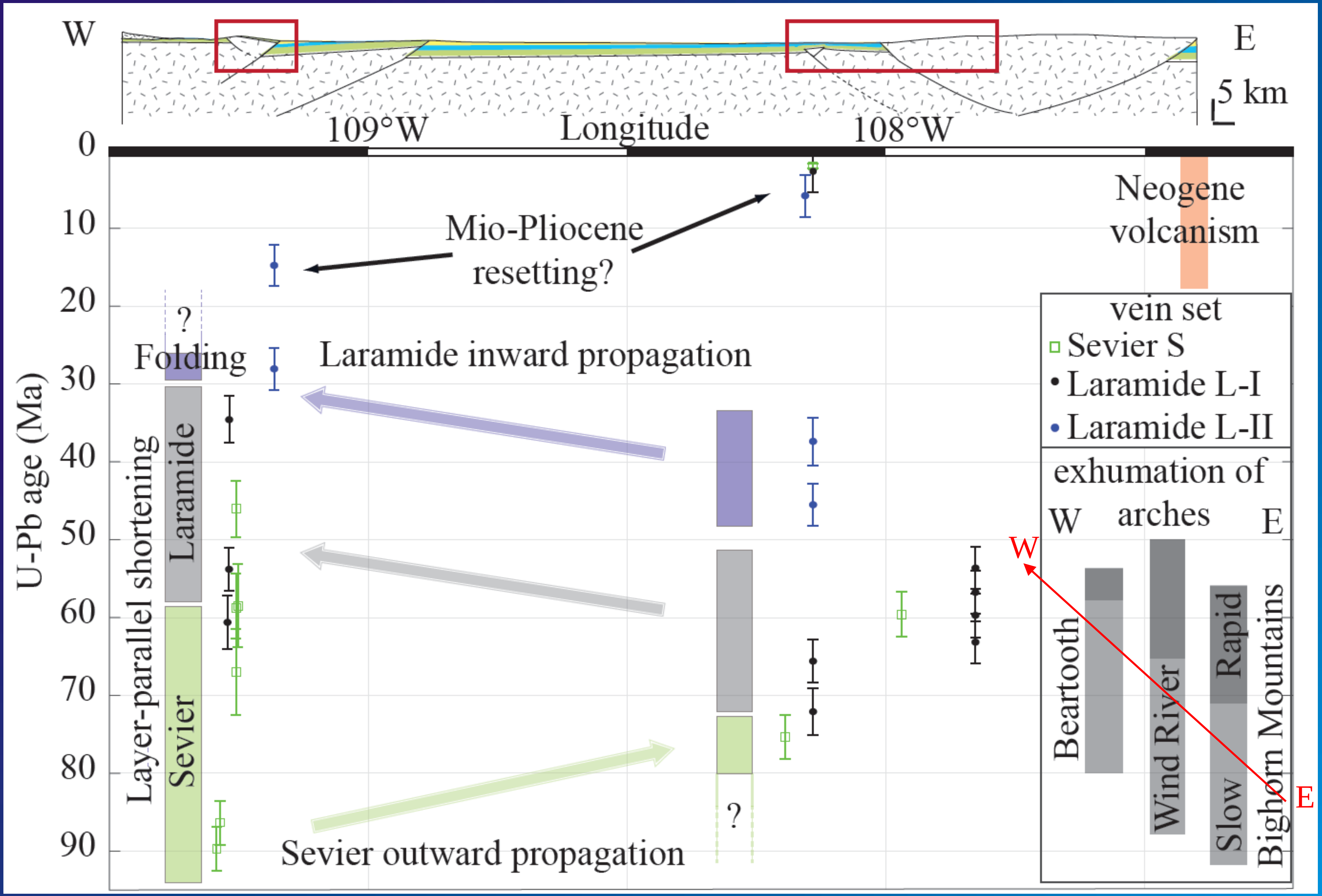

(Beaudoin et al., 2018)

More than 70 samples → only 24 reliable ages !

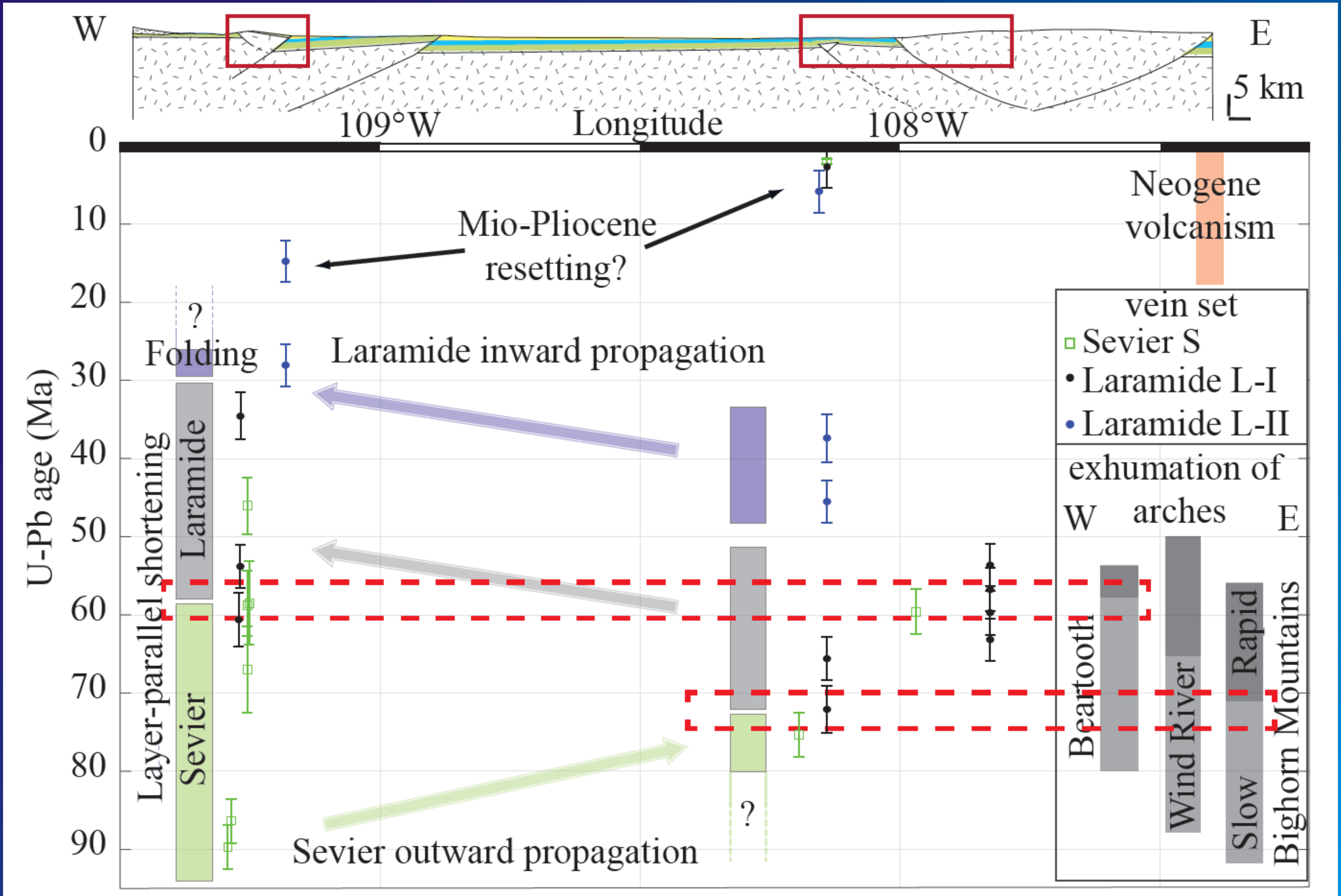

(Beaudoin et al., 2018)

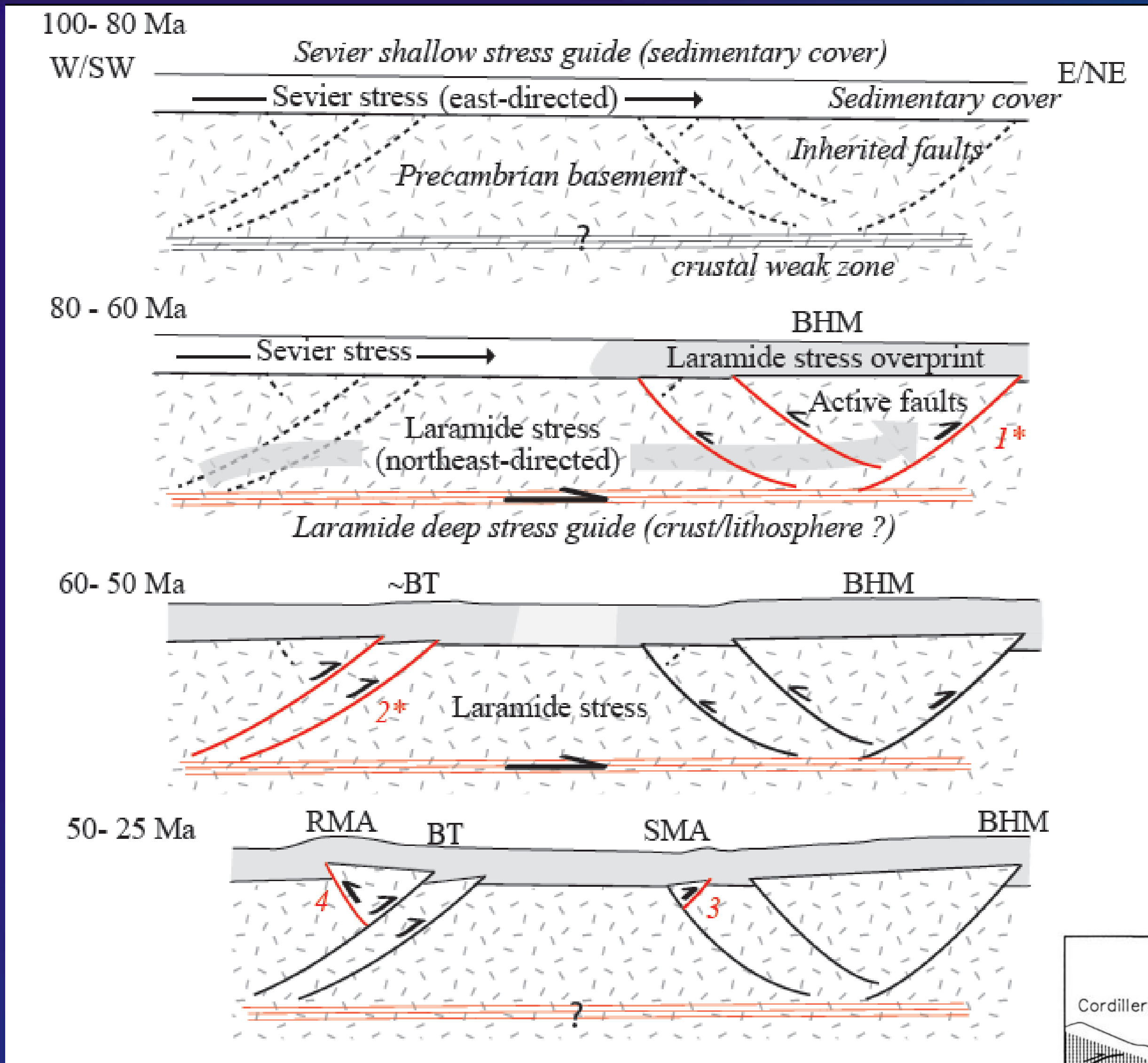

(Beaudoin et al., 2018)

Occurrence of Sevier and Laramide related veins

Time overlap between Sevier and Laramide stress reflects spatial (vertical and horizontal) stress compartmentalization within the basin

Sequential thrust reactivation of inherited basement faults. Delayed vertical transmission of Laramide stress from the basement to the overlying (attached) cover
→ progressive stress loading of the cover

Shallow Sevier stress guide (cover) vs deep Laramide stress guide (crust)

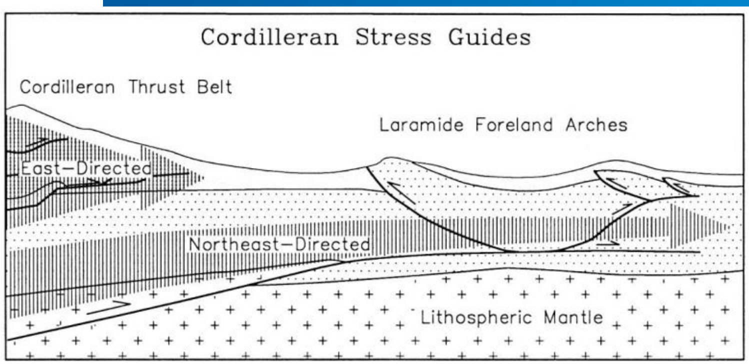

Schematic cartoon showing multiple stress guides and multilevel detachment during Cordilleran-Laramide lateral compression.

(Erslev, 1993)

LA-ICP-MS U-Pb dating of calcite veins in the Bighorn Basin :

-provides absolute time constraints on formation/cementation of systematic vein sets

-confirms the relevance of vein sets to large-scale tectonics

-confirms existing models for propagation of Sevier deformation and for exhumation of Laramide basement-cored structures;

-helps refine age and sequence of activation of individual basement thrusts;

-improves our understanding of stress transmission and build-up throughout the basin.

→ Thin-skinned orogenic wedges develop through a progressive outward (forelandward) stress loading and propagation of deformation through time;

→ Thick-skinned systems show a more erratic sequence owing to the reactivation of basement heterogeneities that govern the stress field in the overlying sedimentary cover.

→ Problem of young (reset) ages from U-Pb dating (calcite, but also U oxides) without any obvious textural evidence for vein re-opening/recrystallization; Role of fluids ?

→ U = very mobile element, current research on what controls U incorporation and "trapping" in carbonates

Etchecopar (1984) and Parlangeau et al. (2018) technique of inversion of calcite twin data for stress

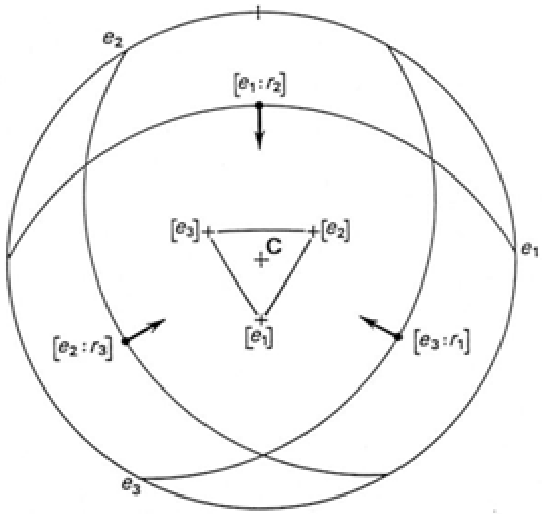

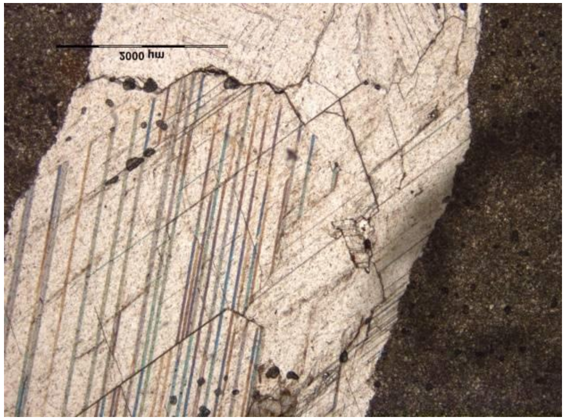

* Orientation of principal stresses
* Differential stress magnitudes

$$(\sigma_1 - \sigma_3) \text{ and } (\sigma_2 - \sigma_3)$$

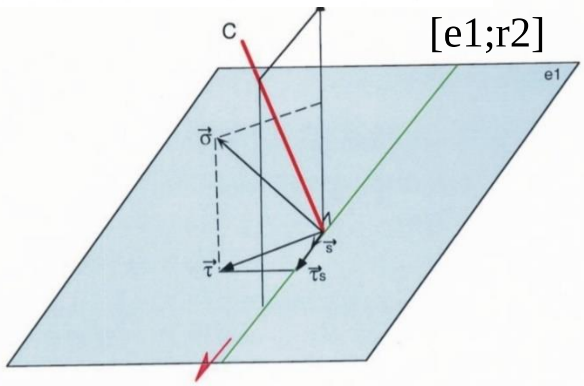

$-(\sigma1-\sigma3)/2 \leq \tau s = (\vec{\sigma}.\vec{s}) \leq (\sigma1-\sigma3)/2$

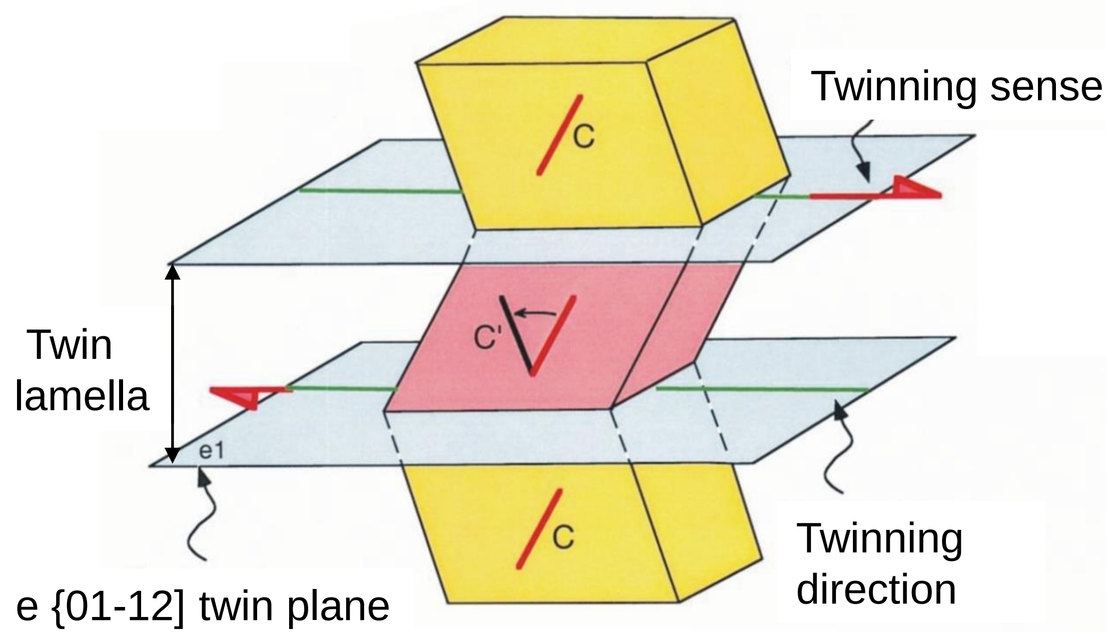

Calcite from S and L-I veins and/or rock matrix

Early-folding and late-folding paleo-differential stress magnitudes from calcite twinning paleopiezometry

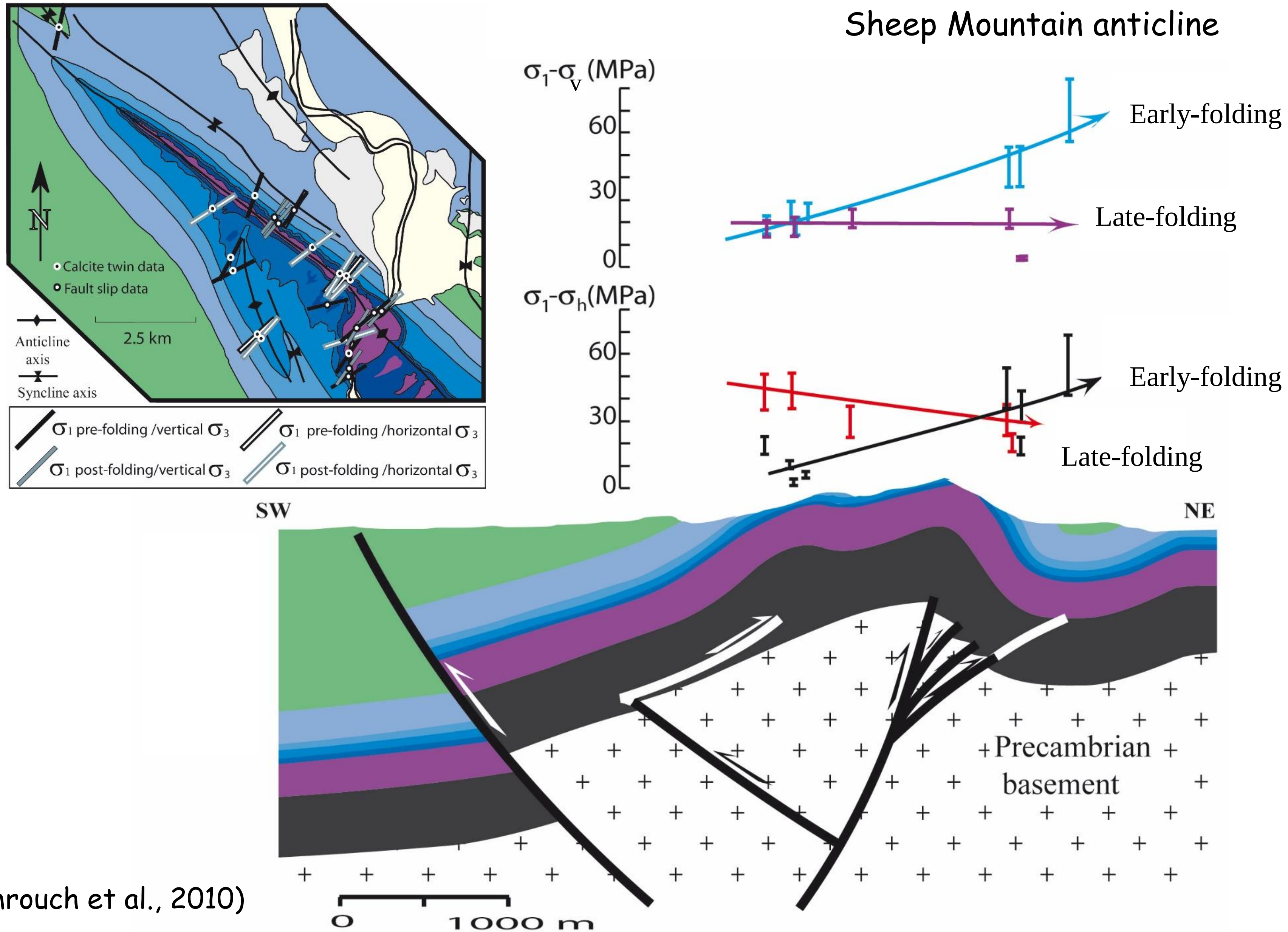

(Amrouch et al., 2010)

Early-folding and late-folding Laramide paleo-differential stress magnitudes from calcite twinning paleopiezometry

(normalization of RMA to same depth than SMA)

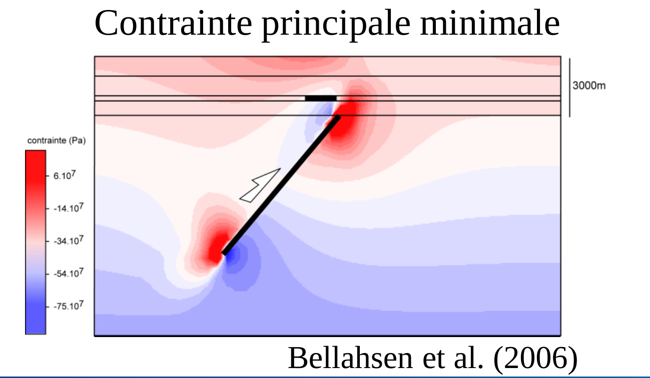

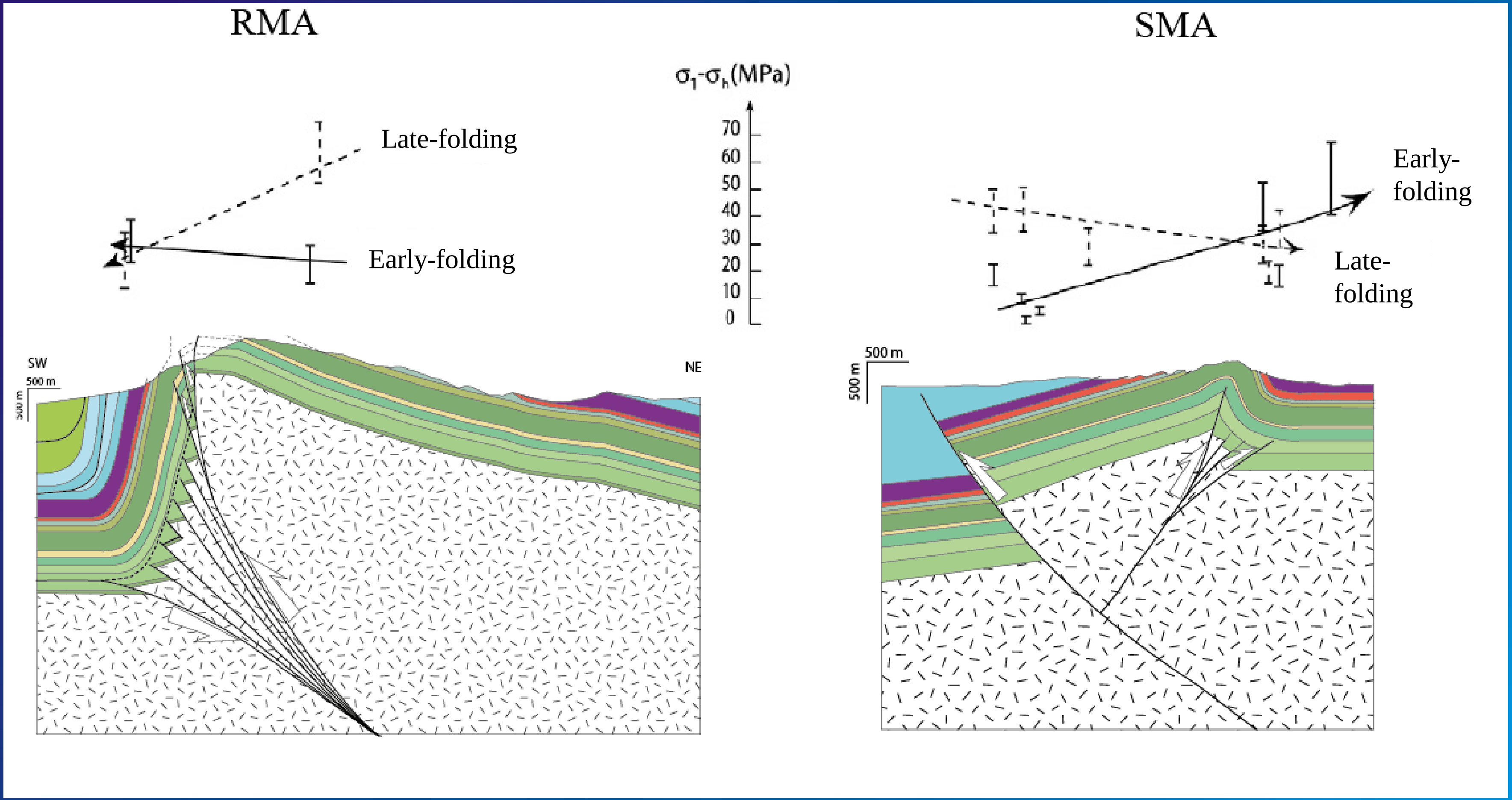

(Beaudoin et al., 2012)

Thermodynamics and kinetics of the growth of a stylolite :

Once dissolution starts, there is a competition between:

- a destabilizing (roughening) force due to pinning particles on the stylolitic surface → resists dissolution in specific locations → increases locally the free energy and produces peaks and teeth.

- two stabilizing (smoothening) forces, long-range elastic forces and local surface tension → tend to reduce the Helmholtz free energy of the solid → flatten the surface by preferentially dissolving areas of local roughness ;

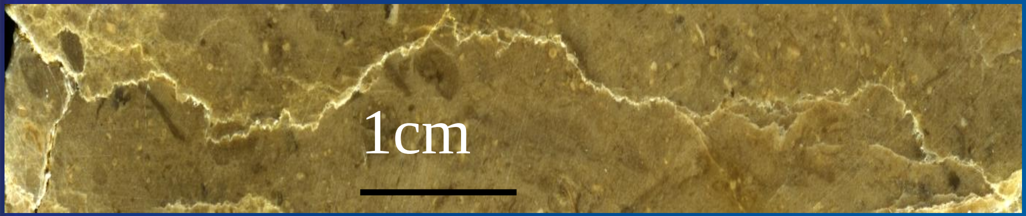

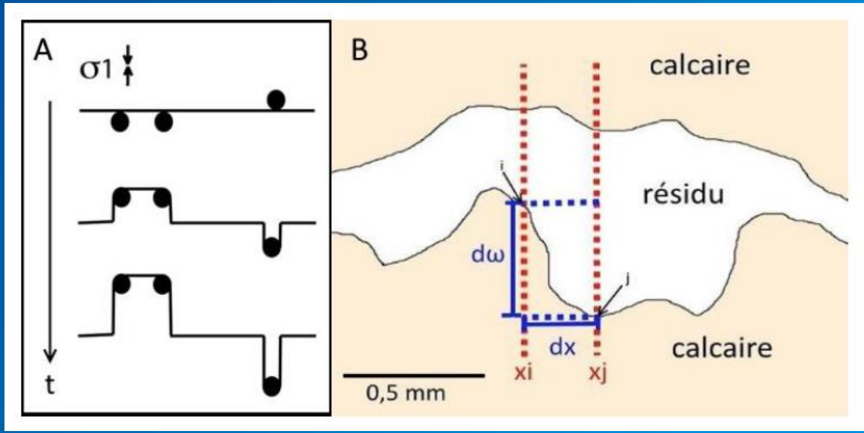

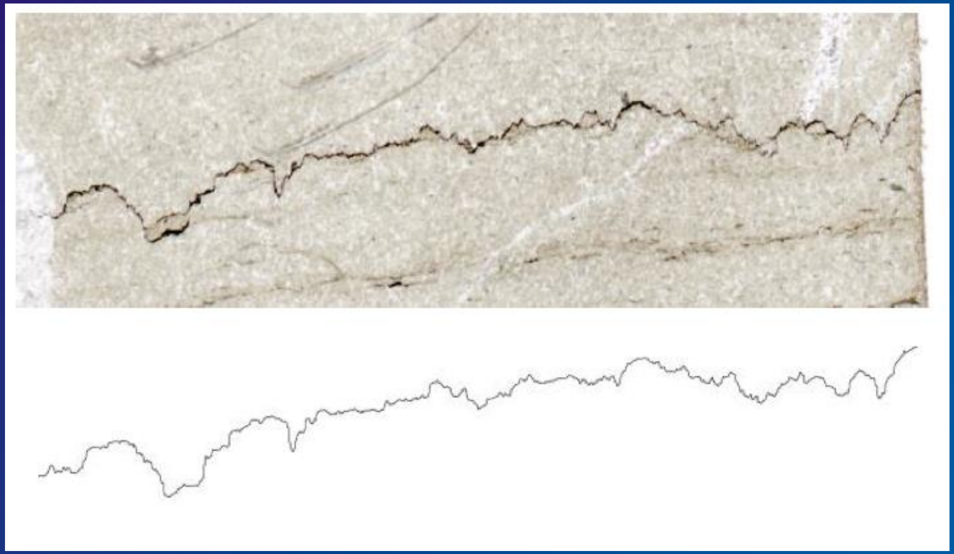

Typical size
5 to10cm

1. Take sample (need to know if they are sedimentary or tectonic)
2. Scan polished surface or thin section (perpendicular to teeth)
3. Extract a complete one-dimensional function

scaling of the roughness

Fourier Power Spectrum

$$P(k) = k^{D-2h}$$

if the signal is self-affine

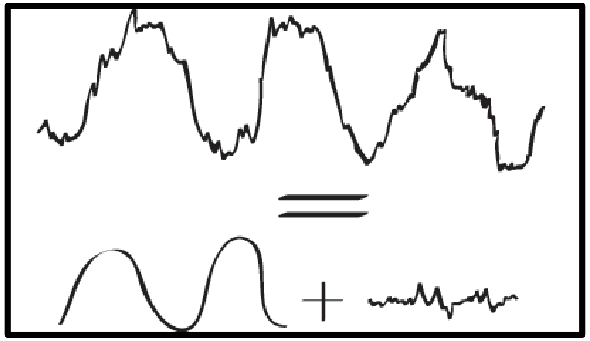

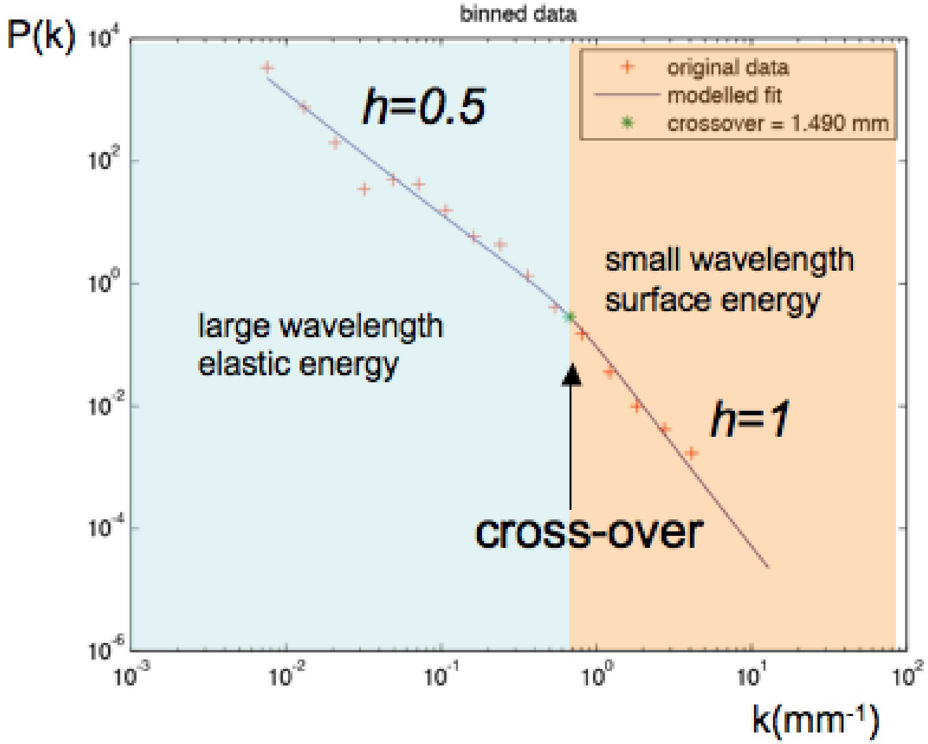

→ two growth regimes (elastic / surface energy dominated regimes), each of those being characterized by a roughness exponent (Hurst exponent) and separated by a crossover length (Lc) that describes the scale at which the switch between regimes of control occurs.

(Schmittbuhl et al., 2004)

$$L_c = \frac{\gamma E}{\beta \sigma_m \sigma_d}$$

γ : surface energy at the solid-fluid interface, E : Young modulus,
$\beta = \nu(12\nu)/\pi$: dimensionless number with ν : Poisson ratio,
σm : mean stress, σd : differential stress.

Considering an isotropic stress in the stylolite plane (sedimentary/bedding-parallel stylolites - BPS) :

$$\left| \begin{array}{l} \sigma_v > \sigma_H = \sigma_h \\ \sigma_H = \sigma_h = \left(\frac{\nu}{1-\nu}\right) \sigma_v \end{array} \right. \rightarrow \left| \begin{array}{l} L_c = \frac{\gamma E}{\beta \alpha {\sigma_v}^2} \\ \alpha = \frac{1}{3} \left(\frac{1+\nu}{1-\nu}\right) \left(\frac{1-2\nu}{1-\nu}\right) \end{array} \right. \rightarrow \left| \begin{array}{l} \sigma_v = \sqrt{\frac{\gamma E}{L_c \beta \alpha}} \\ \sigma_H = \sigma_h = \left(\frac{\nu}{1-\nu}\right) \sigma_v \end{array} \right.$$

This allows to predict the magnitudes of the normal-to-the-plane stress and of the two in-plane stresses

Consistency between maximum burial depth from BPS stylolites and results of basin modelling in the Paris basin

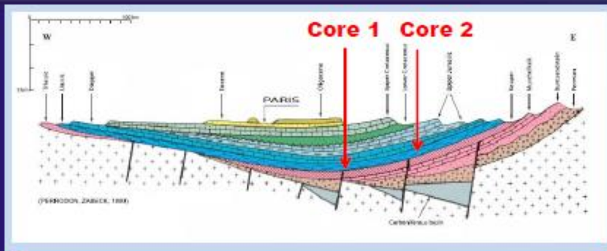

2 Jurassic cores (margin *versus* depocenter) were chosen.

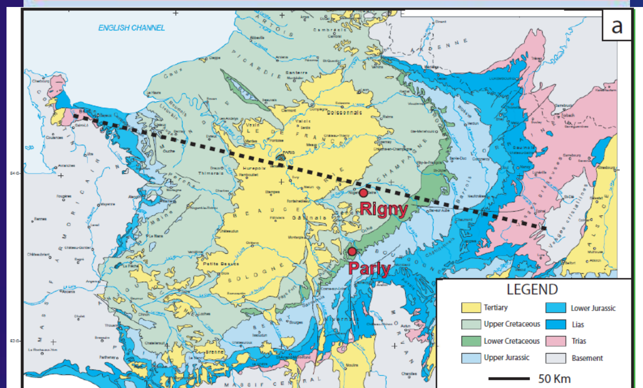

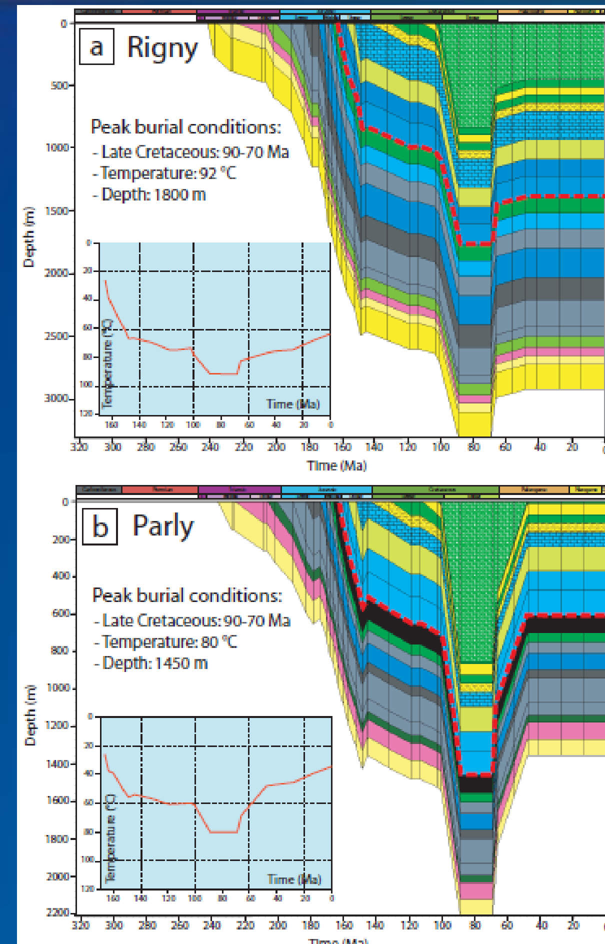

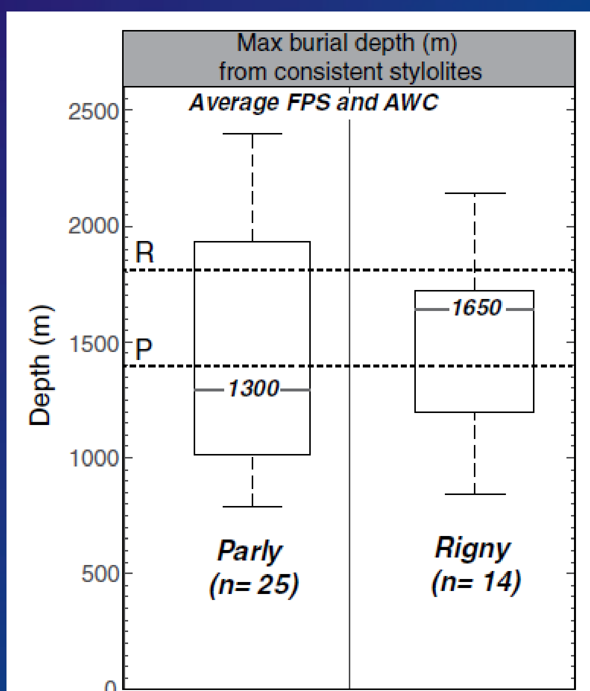

(Beaudoin et al., 2019)

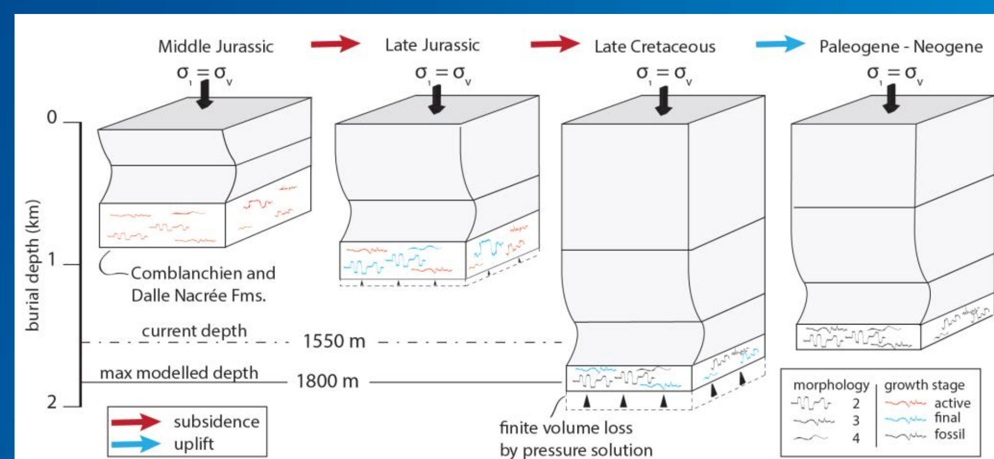

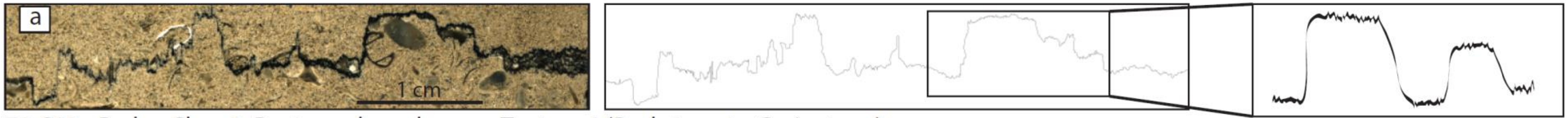

73-S03 - Parly - Class 1: Rectangular columns - Texture 4 (Packstone to Grainstone)

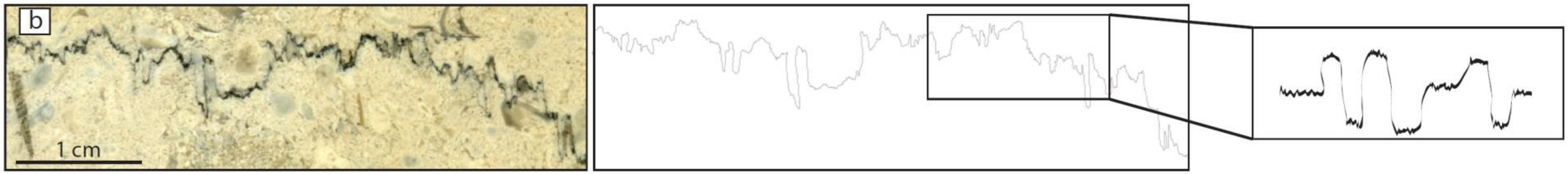

70 -S14 - Parly - Class 2: Seismogram with narrow columns - Texture 3 (Floatstone to Packstone)

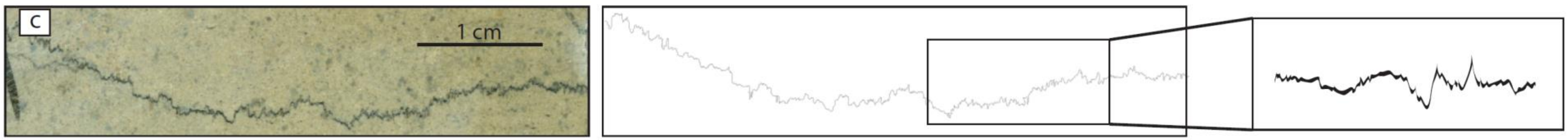

18-S01 - Parly - Class 3: Suture and sharp peak - Texture 2 (Wackstone to Floatstone)

205-S03 - Rigny - Class 4: Simple wave like type - Texture 1 (Mudstone to Wackstone)

Suture and sharp peak BPS (3) are better suited to estimate the real maximum depth, whereas seismogram pinning BPS (2) record preferentially intermediate depths

→ Access to burial (exhumation ?) history in a way independent on assumptions on past geotherm

A tectonic stylolite records a stress anisotropy within the stylolite plane ($\sigma2 \neq \sigma3$) : depending on the orientation the crossover length Lc reflects the differential stress $\sigma1-\sigma2$, $\sigma1-\sigma3$ or a value in between.

If Lc is determined from a 2-D signal, then it depends on the orientation of the cut through the stylolite with respect to $\sigma2$ and $\sigma3$ ($\sigma1$ horizontal and normal to stylolite).

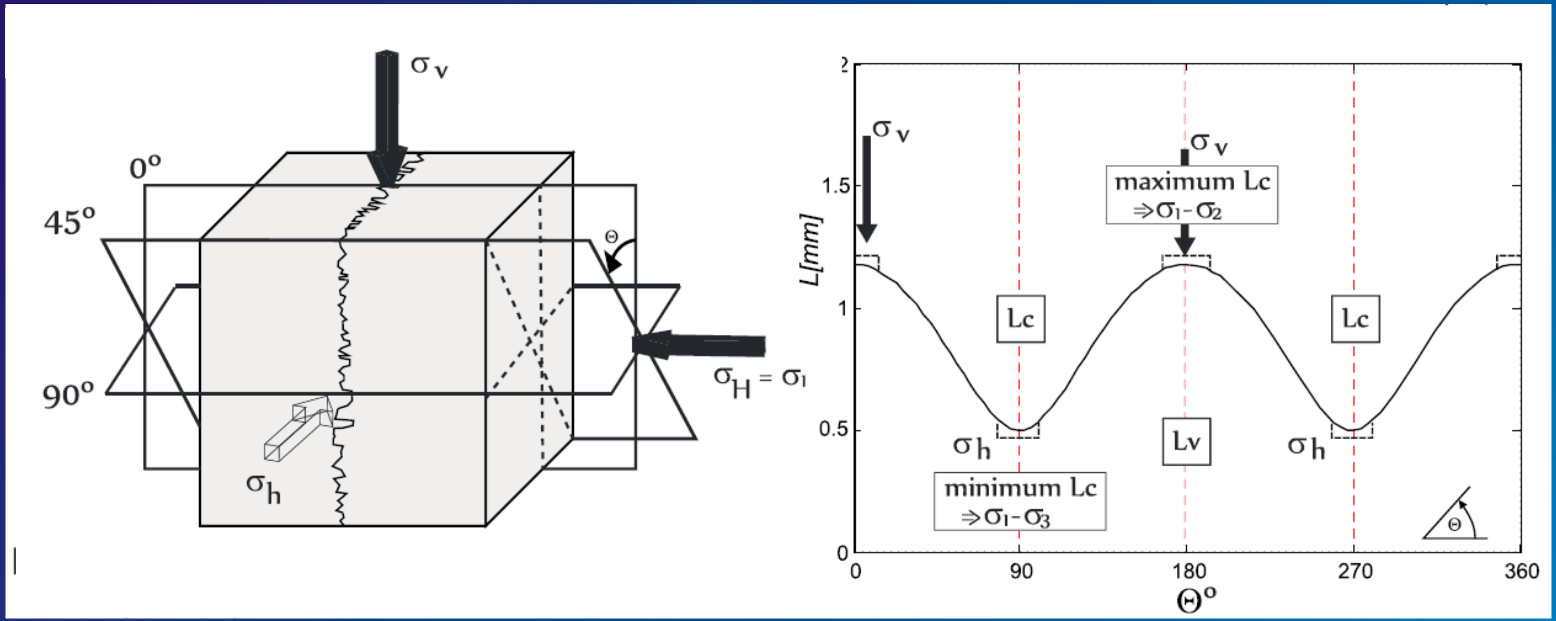

The relationship between Lc and the angle θ is a periodic function, with minimum and maximum Lc separated by 90° → roughness inversion on 2-D scans of 3 surfaces normal to the stylolite yields 3 Lc + the 3 corresponding angles θ between the cuts and the vertical direction.

The minimum and the maximum Lc correspond to ($\sigma1-\sigma3$) and ($\sigma1-\sigma2$). If θ associated with Lcmin is close to 0°, then $\sigma2$ is vertical (SS regime); otherwise, if θ associated with Lcmax is close to 0°, then $\sigma3$ is vertical (R regime).

Stylolite Roughness Inversion Technique (SRIT) works for :

- Stress direction
- Depth of sedimentary stylolites (from shallow to 4000m)
- Tectonic stylolites (needs 3D and assumption of depth)

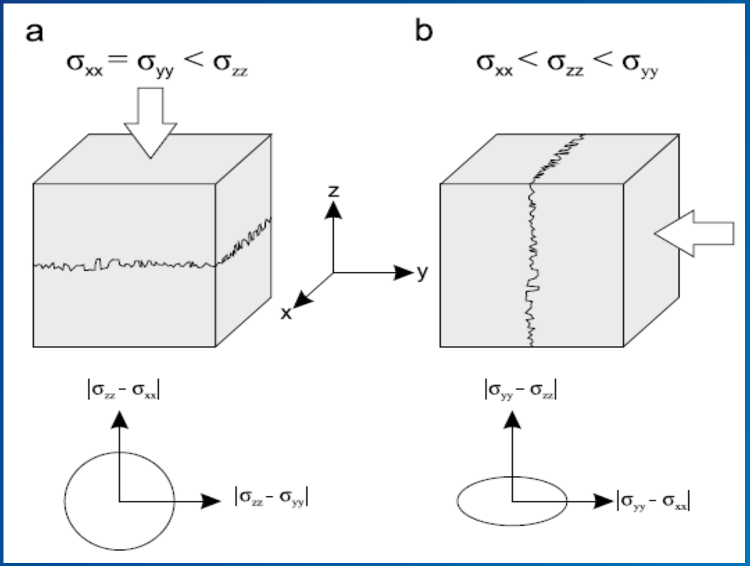

Sedimentary stylolites	Tectonic stylolites
$\sigma_z^2 = \frac{\gamma E}{\alpha\beta L_c}$	$\sigma_y = f(\frac{L_v}{L_h}; \sigma_z) \pm \sqrt{\Delta(\frac{L_V}{L_h}, \sigma_z, \frac{a}{L_h})}$
$\sigma_x = \sigma_y = \frac{\nu}{1-\nu}\sigma_z$	$\sigma_x = \sigma_y - \frac{L_V}{L_h}\sigma_y - \frac{L_V}{L_h}\sigma_z$

Combining stylolite roughness and calcite twinning paleopiezometry reveals the complexity of progressive stress patterns during folding (Monte Nero anticline, Apennines, Italy)

(Beaudoin et al., 2016)

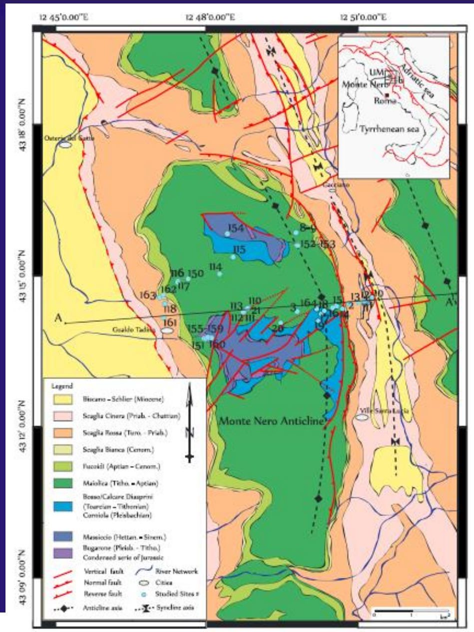

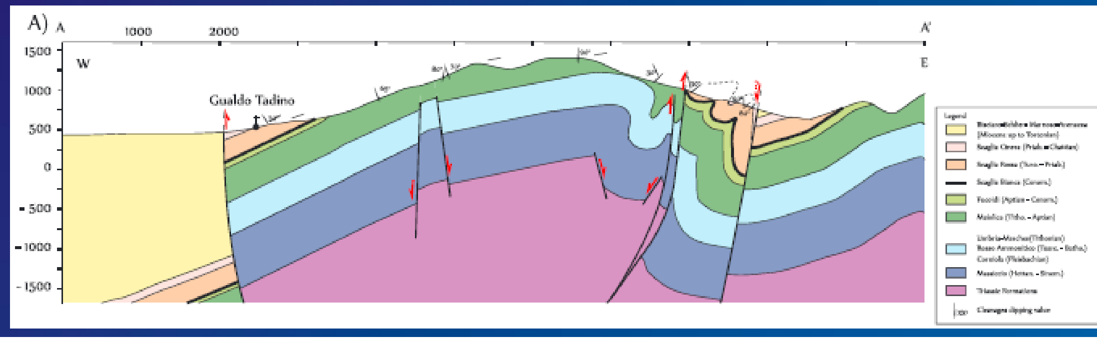

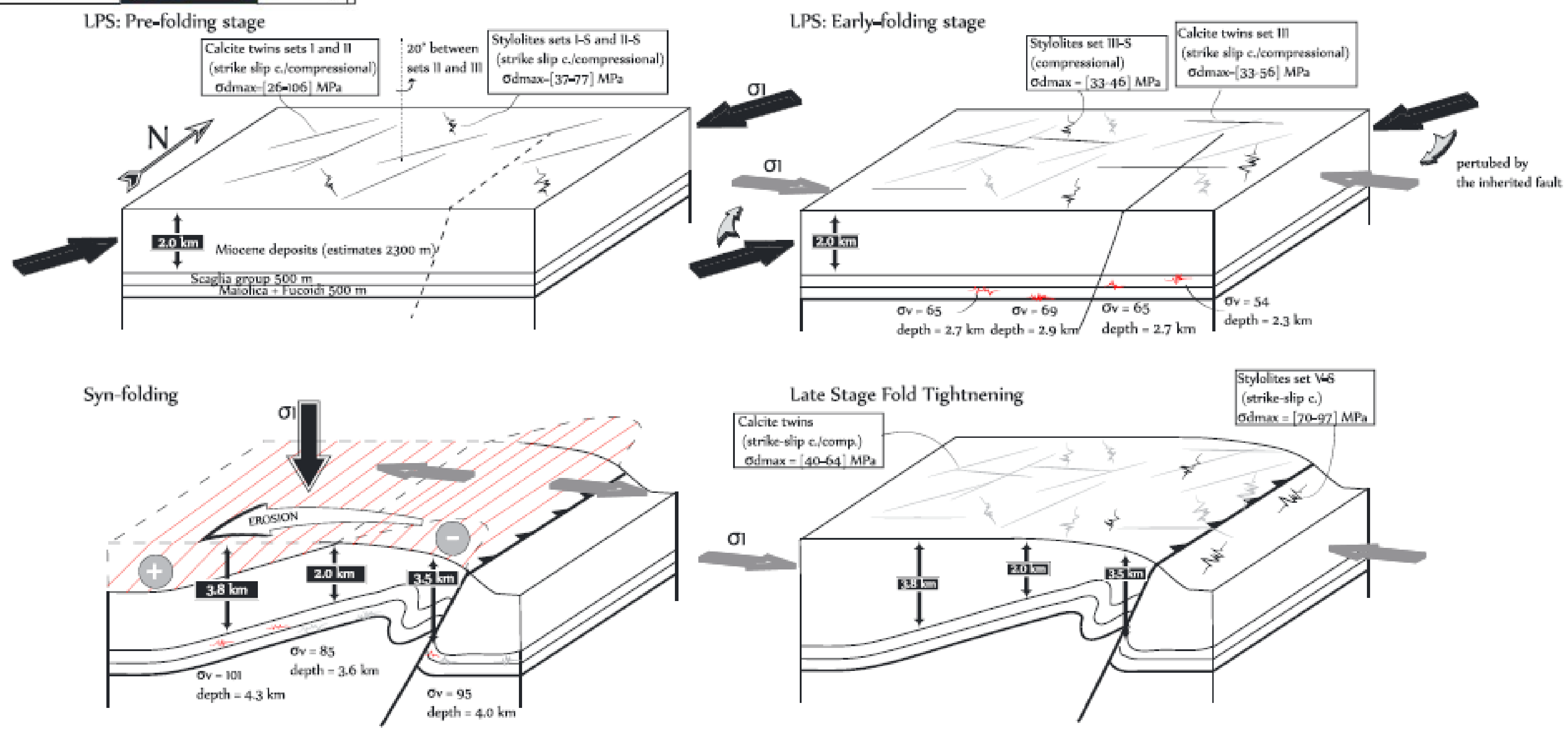

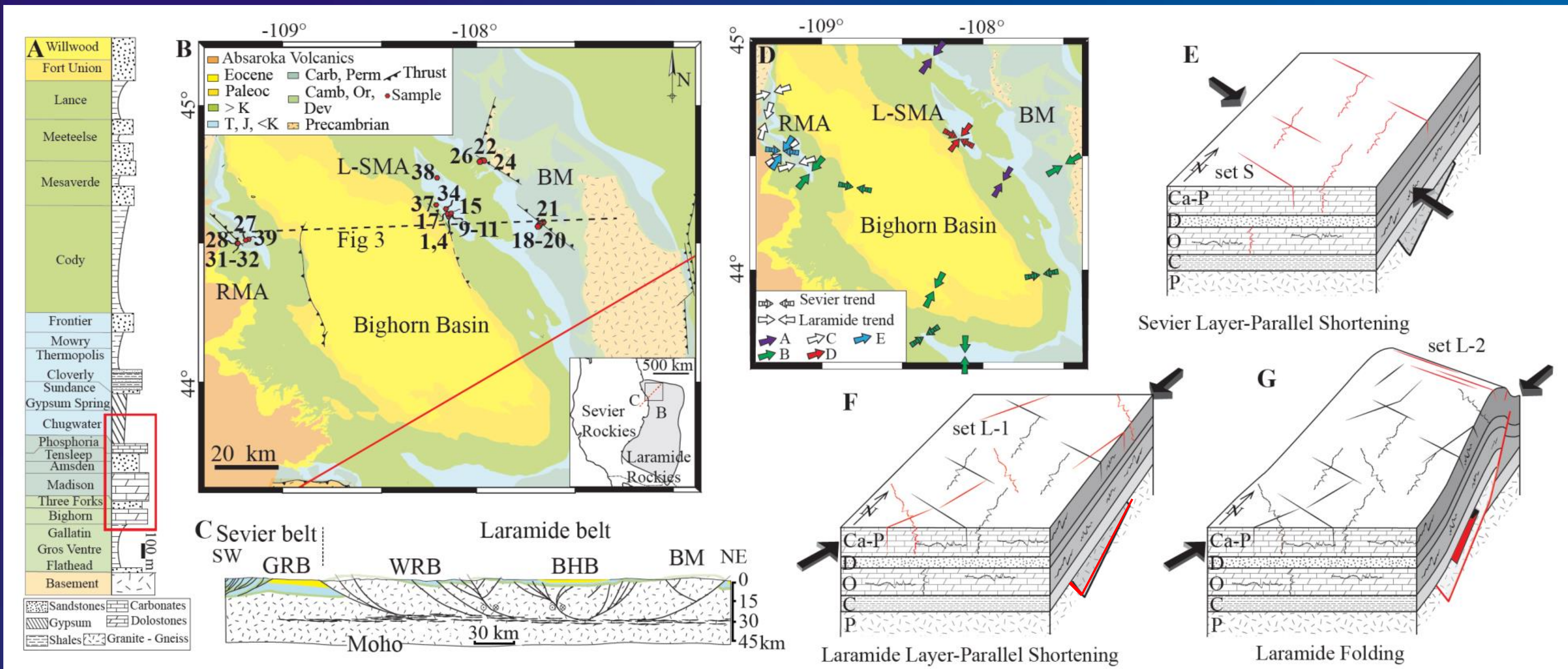

(Beaudoin et al., submitted)

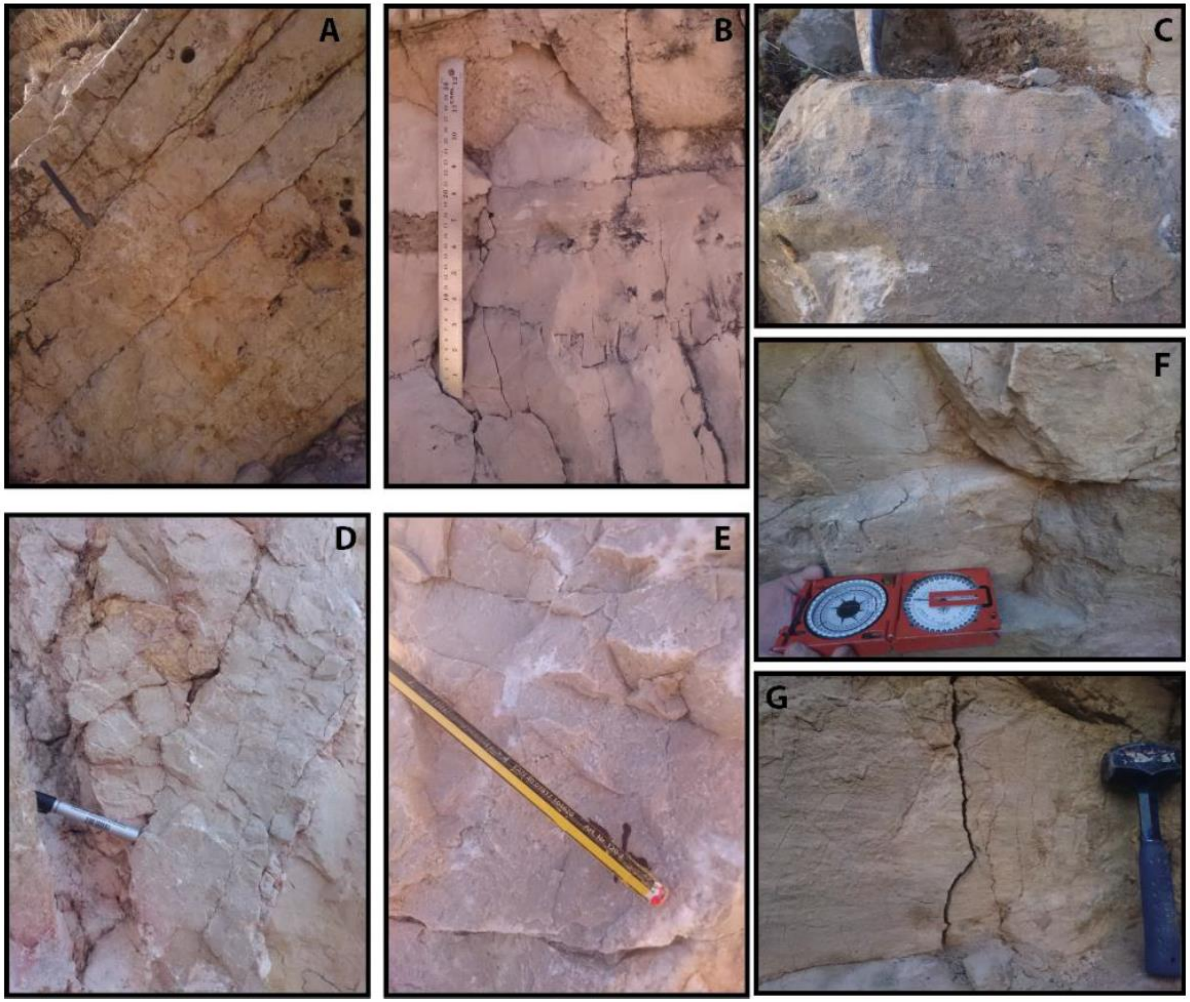

Fig S-1: Field photographs of bedding-parallel stylolites (A-D) and tectonic stylolites (E-G) from studied anticlines: Rattlesnake Mountain (A, E), Sheep Mountain (B), Bighorn Mountain (D, F, G), Little Sheep Mountain (C).

(Beaudoin et al., submitted)

BPS RMA

BPS LSMA

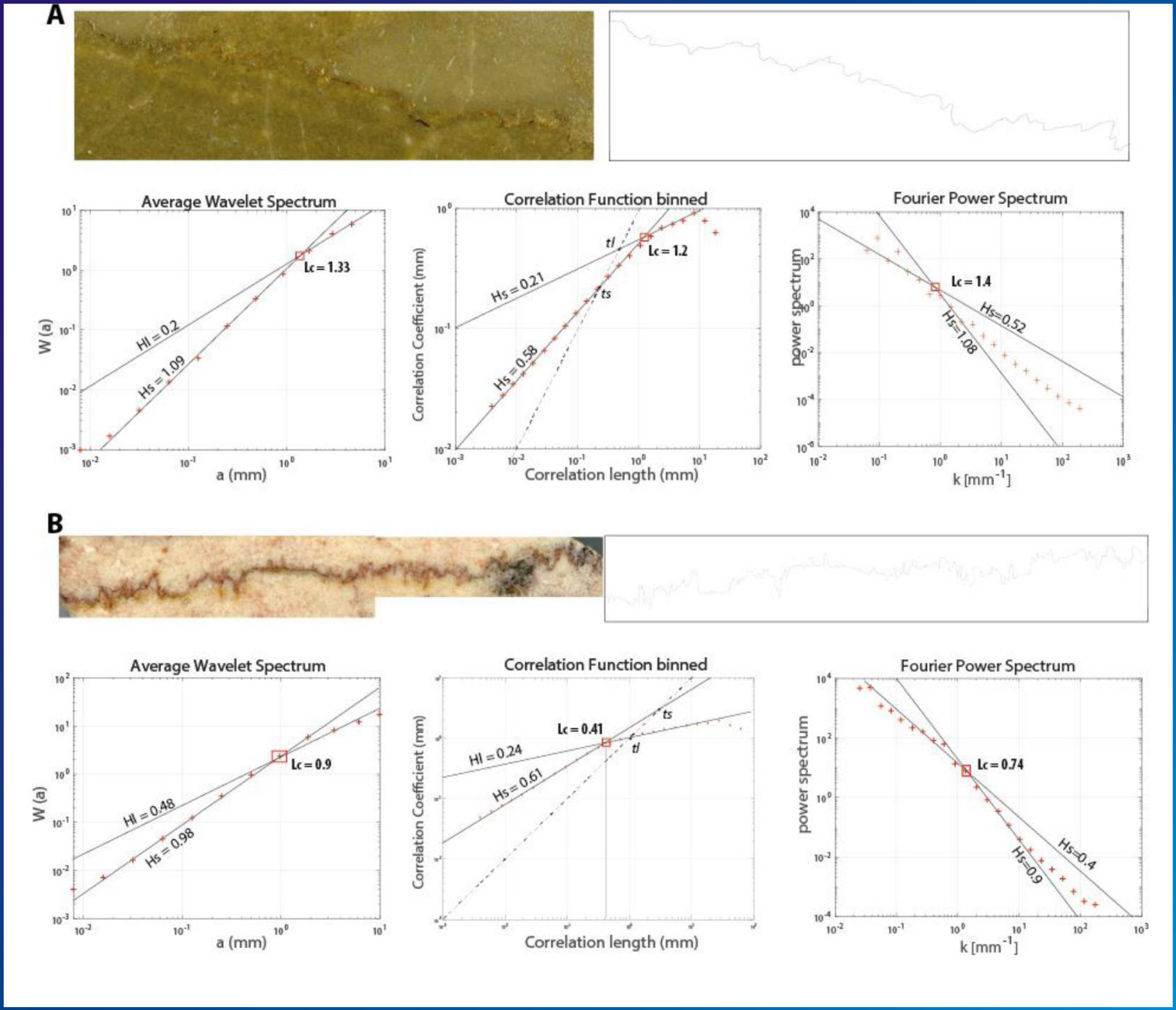

(Beaudoin et al., submitted)

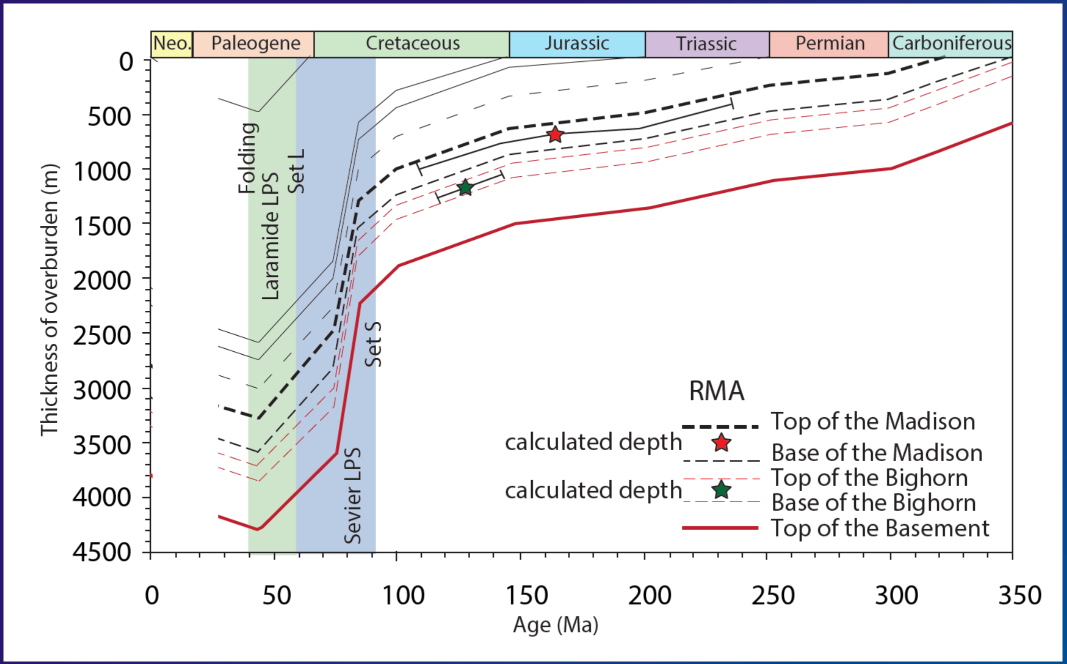

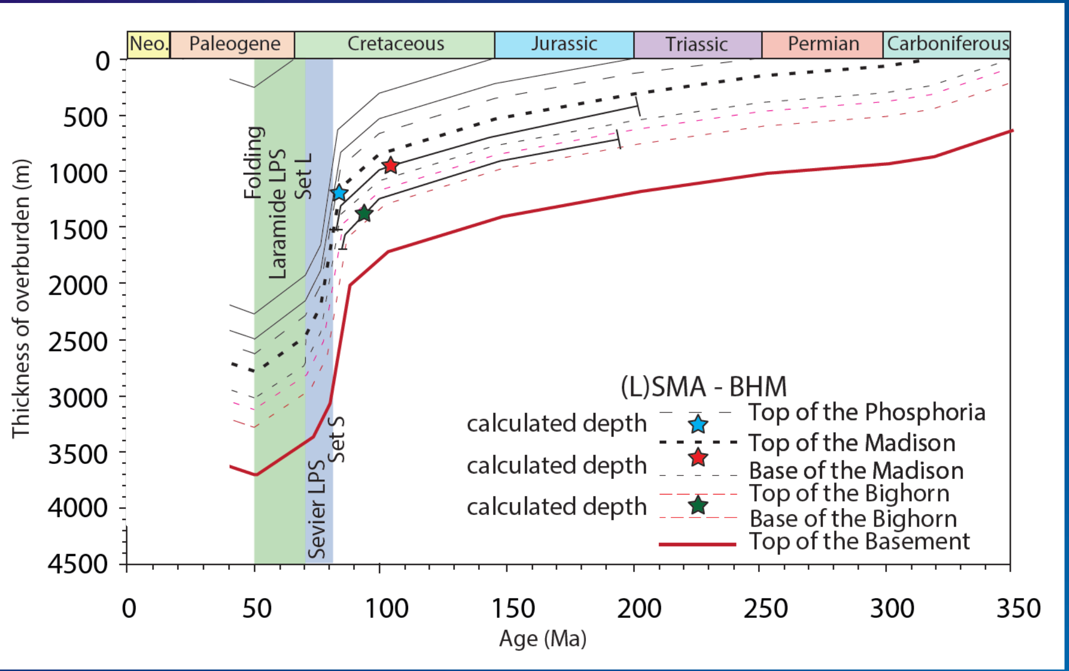

Depth calculated from BPS is always lower than the maximum depth predicted by the sediment thickness

Vertically-oriented pressure-solution was active to accommodate burial until mid- to late-Cretaceous times

BPS-related maximum depth lower than the estimated depth at which the Sevier systematic vein set started to develop

BPS stopped being active when σ_1 switched from vertical to horizontal; Veins formed under horizontal σ_1

(Beaudoin et al., submitted)

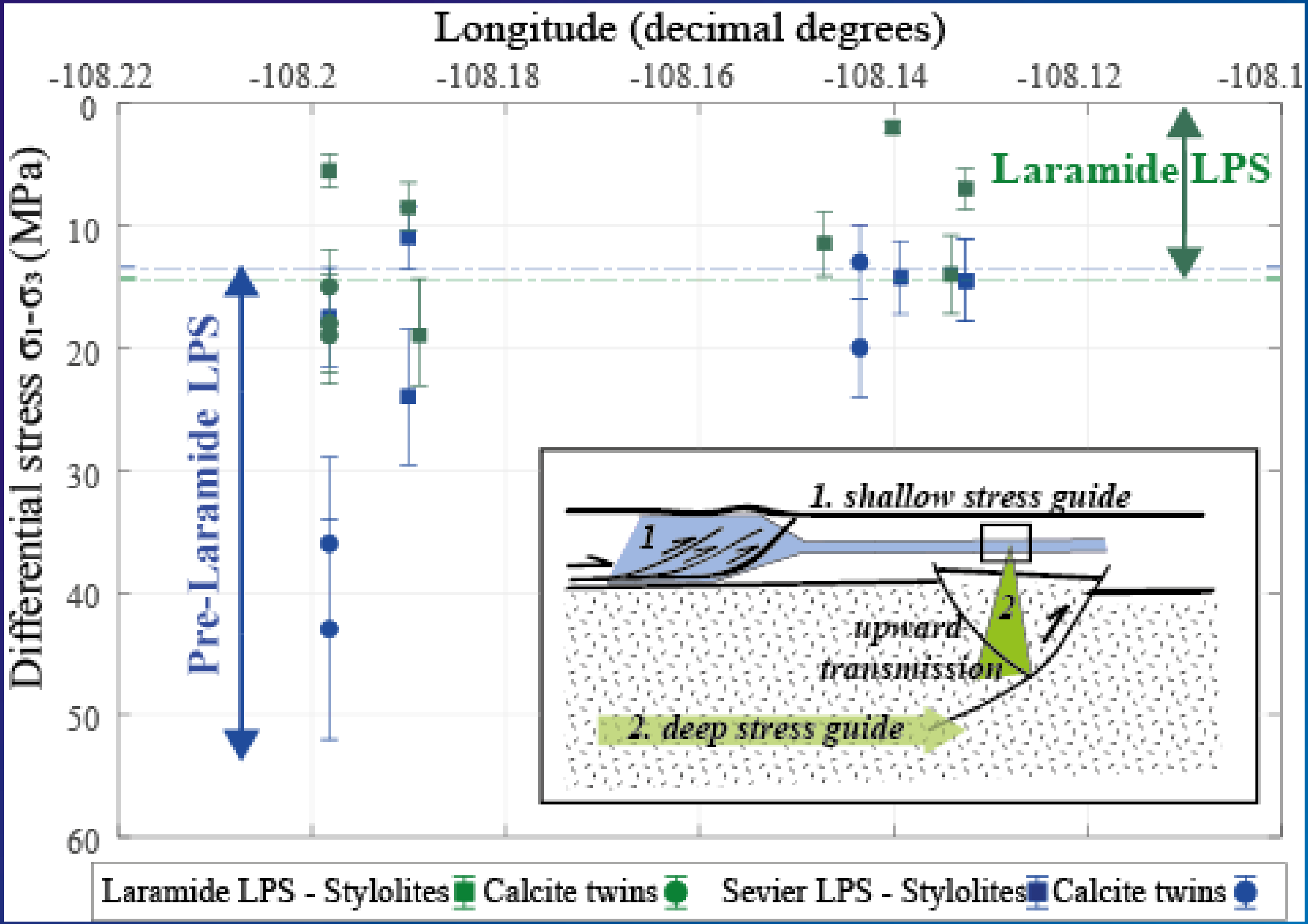

(Beaudoin et al., submitted)

Eastward decreasing Sevier differential stress magnitudes (?)

Sub-constant low Laramide differential stresses

Vertical transmission of Laramide stress from the basement to the overlying (attached) cover → progressive Laramide stress imprint (cf U-Pb)

→ Shallow Sevier stress guide (cover) vs deep Laramide stress guide (crust)

→ stress magnitudes in the cover mainly controlled by local (basement) structures during thick-skinned tectonics rather than by the distance to the orogenic front as in thin-skinned tectonics.

Influence of the structural style on orogenic stress transmission into forelands

Take-home message

Conclusions

Integrated picture of stress evolution (before and) during (thick-skinned) folding from the local scale to the basin scale.

Stylolites : a new efficient paleopiezometer available for the shallow crust.

Direct calcite age dating → requires numerous samples and works when you are lucky !

Improved understanding of the sequence of deformation and stress distribution in polyphase orogenic forelands

Interest of multi-techniques/scales approach and relevance of micro/meso-scale deformation features to large-scale tectonics

Thank you for inviting me…